ISAS - INTERNATIONAL SCHOOL
FOR ADVANCED STUDIES

ATTESTATO DI RICERCA

"Magister Philosophiae"

THE SYNCHROTON SELF COMPTON MODEL FOR COMPACT SOURCES: SELF CONSISTENT SOLUTIONS FOR CONTINUOUS INJECTION INCLUDING PAIR PRODUCTION

CANDIDATO:

Gabriele Ghisellini

RELATORI:

Marek Abraomowicz

Roland Svensson

a.a. 1985/86

TRIESTE

ISSA - SCUOLA
TERNAZIONALE
SUPERIORE
STUDI AVANZATI
TRIESTE
Strada Costiera 11

ISAS - INTERNATIONAL SCHOOL FOR ADVANCED STUDIES

OCTOBER 1986

THE SYNCHROTRON SELF COMPTON MODEL FOR COMPACT SOURCES: SELF CONSISTENT SOLUTIONS FOR CONTINUOUS INJECTION INCLUDING PAIR PRODUCTION

Thesis submitted for the degree of Master of Philosophy

CANDIDATE:

Gabriele Ghisellini

SUPERVISORS:

Marek A.Abramowicz
Roland Svensson

Table of contents

Introduction	Page	1
Chapter 1: The standard SSC model	"	3
1.1 Cooling timescale	"	4
1.2 The continuity equation	"	5
1.3 Emissivities	"	7
1.4 Diagnostic	"	8
1.5 Predictions	"	9
1.6 Prescriptions	"	11
Chapter 2: The SSC model revisited	"	13
2.1 The continuity equation	"	13
2.2 The "X-ray excess"	"	14
2.3 The "Klein Nishina dimming"	"	17
2.4 The case of steep injection	"	20
2.4a Determination of α_γ	"	23
2.4b Determination of α_c	"	24
2.4c Effects of cool particles	"	25
2.4d Comparison with numerical results	"	26
Chapter 3: The importance of pair production in non-thermal models	"	32
Chapter 4: Pair production in SSC models	"	39
4.1 The problem	"	40
4.2 The case of one generation of pairs	"	41
4.2a The model	"	41
4.2b Effects of thermal pairs	"	44
4.2c An example	"	45
4.2d Discussion	"	49
Conclusions	"	52

Introduction

The general features of the synchrotron self Compton (SSC) model and its relevance for active galactic nuclei (AGNs) have been well established soon after the discovery of quasars and the conviction of their extragalactic nature. Now the SSC is one of the most popular non thermal model to interpret the overall emission of AGNs. Synchrotron radiation can in fact easily produce power law spectra, radio emission, and polarization, frequently observed in these objects. Furthermore, their compactness, as deduced from time variability or directly measured by VLBI techniques, makes the inverse Compton process a very efficient radiation mechanism. Thus, photons produced from radio to optical frequencies by relativistic electrons via the synchrotron process can be boosted at X and γ-ray energies by the same electrons via the inverse Compton mechanism.

In this thesis, I will present some new results concerning the SSC model when applied to compact sources. Here compact means a luminosity to size ratio L/R exceeding 10^{28} erg $s^{-1}cm^{-1}$. In this case, the cooling time of the radiating electrons is shorter than any other relevant timescale. New relativistic electrons are assumed to be continuously injected throughout the source without being reaccelerated. The consequences of the two main opacity processes: synchrotron self absorption and γ-ray absorption, are investigated, finding in several cases analytical solutions for the emitted spectrum.

In Chapter 1 the standard SSC model is reviewed, as formalized in the classical paper of Jones, O'Dell and Stein (1974), but using a different notation. The main results derived in the past using this model are then briefly discussed.

In Chapter 2, some of the simplifying hypotheses of the

standard model are relaxed. In fact, the steady energy density of the relativistic electrons is not assumed, but derived, taking into account synchrotron self-absorption and the decreased cooling of the electrons radiating in the Klein Nishina regime. A clear distinction between flat and steep power law injection is made, where flat here means that the bulk of the injected power is in high energy electrons. Since the opposite case requires a different approach, it is discussed separately in the second part of the chapter. Contrary to what derived in the standard model, it is found that synchrotron and inverse Compton spectra can have different slopes in both (steep and flat) injection cases. Furthermore, in the case of steep injection, the spectral index of the emission spectrum is no more related to the electron injection slope, and cannot be steeper than unity.

In Chapters 3 and 4, I examine the importance of γ-ray absorption and electron positron pair production. They have been recently studied by many authors in the context of a non thermal, although not SSC, model. Their main results are reviewed in Chapter 3, since they can have important application also in the SSC model.

Finally, a simplified and analytical SSC model including pair production is presented in Chapter 4, where its possible relevance for the interpretation of variability in AGNs is discussed.

1. The standard synchrotron self Compton model

A relativistic electron of energy γmc^2 and Lorentz factor γ spiraling in a magnetic field B emits a power

$$P_s = (4/3)\sigma_T c \gamma^2 U_B \qquad 1.1$$

where σ_T is the Thomson cross section, U_B is the magnetic energy density, and where an isotropic electron distribution is assumed. This power peaks at an energy (in units of mc^2)

$$x_s = h\nu_s/(mc^2) = (4/3)\gamma^2 x_B \qquad 1.2$$

where $x_B=B/B_c$ $\left(B_c=m^2c^3/(\hbar e)\cong 4.4\times10^{13}\ G\right)$ is the Larmor dimensionless energy.

One can think of the synchrotron process in terms of a scattering between the electrons and the virtual magnetic photons of energy x_B (Blumenthal and Gould 1970). Indeed, if we replace U_B with the photon energy density U_r and x_B with x_s we obtain the power emitted by the IC process in the Thomson regime

$$P_c = (4/3)\sigma_T c \gamma^2 U_r \qquad 1.3$$

and the energy where this power peaks

$$x_c = (4/3)\gamma^2 x_s \qquad 1.4$$

This is strictly true only for $\gamma x_s << 3/4$, where the Thomson cross section can be used. For $\gamma x_s > 3/4$, in the rest frame of the electron the incoming photon has more energy than the electron rest mass, and recoil is important. The energy of the scattered photon is then of the same order of the electron, independently of the incoming photon energy. The process becomes less and less probable as γx_s increases, due to the decline of the Klein Nishina cross section, which

must be used in this case. So, despite the high energy transfer in each interaction, the IC radiation in the Klein Nishina regime ($\gamma x > 3/4$) can usually be neglected. This means that if the synchrotron spectrum of a source is broad enough, not all its radiation energy density is available for scattering, but only that part below the Klein Nishina limit. In eq. 1.3 U_r becomes function of γ, and the emitted power is no more proportional to the square of the energy. As we shall see in the next chapter, this can have important consequences when deriving the steady distribution of the relativistic electrons.

1.1 Cooling timescale

Defining $t_{cool} = |\gamma/\dot{\gamma}|$ we have

$$t_{cool} = \frac{\gamma}{\frac{4}{3}\frac{\sigma_T c}{mc^2}\gamma^2 (U_B + U_r)} \qquad 1.5$$

where U_r can be related to the luminosity and the size of the source

$$U_r = (3/4)(R/c)3L/(4\pi R^3) \qquad 1.6$$

where R/c is the light crossing time, and the factor 3/4 accounts for spherical symmetry. Defining $R=10^{15}R_{15}$, $L=10^{45}L_{45}$

$$t_{cool} \cong \frac{5165}{\gamma} \frac{R_{15}^2}{L_{45}\left[U_B/U_r + 1\right]} \text{ s.} \qquad 1.7$$

which is extremely short, compared to the crossing time, $t_{cross} \cong 3\times10^4 R_{15}$ s, even for electrons of $\gamma=1$.

1.2 The continuity equation

A continuously injected distribution of relativistic electrons will reach a steady density distribution in a time t_{cool}, following the continuity equation

$$\frac{dN(\gamma)}{dt} - \frac{d}{d\gamma}\left(\dot{\gamma}\, N(\gamma)\right) = Q(\gamma) \qquad 1.8$$

where the source function $Q(\gamma)$ is the injection rate of electrons with energy γmc^2. Solving for steady state we have

$$N(\gamma) = -\dot{\gamma}^{-1} \int_{\gamma}^{\gamma_{max}} Q(\gamma')\, d\gamma' \qquad 1.9$$

For power law injection $Q(\gamma)=A\gamma^{-s}$, $s>1$, complete Thomson cooling, and neglecting synchrotron selfabsorption (to be discussed later) the distribution $N(\gamma)$ becomes

$$N(\gamma) = K\gamma^{-(s+1)}, \quad \gamma < \gamma_{max} \qquad 1.10$$

while, in the case of monoenergetic injection, $Q(\gamma) = A\delta(\gamma-\gamma_{max})$

$$N(\gamma) = K\gamma^{-2}, \quad \gamma < \gamma_{max} \qquad 1.11$$

and, in general, this is the flattest slope we can obtaine in this simple model (but see next chapter). This slope can be obtained also for $s<1$ and large γ_{max}. The constant K is the total number density of relativistic electrons (apart a factor of order unity) and can be shown to be

$$K = \frac{1}{\sigma_T R} \begin{cases} \dfrac{2-s}{s-1} \dfrac{U_r}{U_B+U_r} \dfrac{1}{\gamma_{max}^{2-s}-1}, & s>1,\ s\neq 2 \qquad 1.12a \\ \dfrac{U_r}{U_B+U_r} \dfrac{1}{\gamma_{max}}, & s<1 \qquad 1.12b \end{cases}$$

Large γ_{max} (for $s<2$) means low K, since the the bulk of the energy is carried by few electrons. For $s>2$, all the energy

is in low energy particles, and K does not depend on γ_{max}.

Note that we can define a Compton optical depth

$$\tau_c = \sigma_T K R \qquad 1.13$$

As can be seen, τ_c is always smaller than unity, and represents the fraction of photons that can be scattered by the relativistic electrons. Scattering of the virtual quanta of the magnetic field by power law electrons will originate a power law synchrotron spectrum proportional to τ_c, while the first order IC spectrum will depend on τ_c^2, the second order on τ_c^3, and so on, until the Klein Nishina regime is reached.

It is important to stress that eqs. 1.11, 1.12 are the self-consistent solution of eq. 1.9, in the case of complete Thomson cooling and negligible selfabsorption effects. In this case U_r can be expressed in terms of the luminosity and size only, and eq. 1.9, in general an integral equation, (U_r depends on the integral of $N(\gamma)$, $N^2(\gamma)$, and so on, over γ) becomes linear. A similar result was obtained by Zdziarski and Lightman (1985) who considered the radiation energy density of only the synchrotron photons, deriving a quadratic equation for U_r^s.

From eq.1.12a, with s>2, we have

$$K \cong \frac{1}{\sigma_T R} \frac{s-2}{s-1} \frac{U_r}{U_r + U_B} \qquad 1.14$$

so that equal sized, weakly magnetized, steep spectrum sources have the same number density of electrons, irrespective of γ_{max} and of the injection rate of electrons (or, equivalently, of luminosity). It follows that for these sources, also the ratio between the synchrotron and first order Compton flux density at a given frequency is fixed, and close to unity. It is worth noting, from eq. 1.12a, that K is limited. In fact, fixing R, and s>2, the relativistic electron density is initially proportional to the injection

rate. As U_r becomes greater than U_B, the term $U_r/(U_r+U_B)$ approaches the limiting value of unity, so the electron density becomes independent on the number of electrons injected in the source, since in this case the enhanced cooling balances the increased injection. Taking into account synchrotron self absorption will strengthen this statement, making it valid for any value of U_B/U_r, as will be shown in the next chapter.

1.3 Emissivities

Assuming that all the power emitted by the single electron is concentrated at the peak of the emission (δ-function approximation) it is straightforward to derive the synchrotron and the IC emissivities, for a power law distribution of relativistic electrons.

For synchrotron

$$\varepsilon_s(x_s) = \frac{\sigma_T c}{16\pi}\left(\frac{4}{3}\right)^{\alpha} B_c^{1-\alpha}\, K B^{1+\alpha}\, x_s^{-\alpha} \qquad 1.15a$$

$$= \left(\frac{4}{3}\right)^{\alpha} \frac{\tau_c}{2}\,\frac{1}{R/c}\,\frac{U_B}{x_B}\,\left(x_s/x_B\right)^{-\alpha} \qquad 1.15b$$

where the spectral index $\alpha=s/2$. In the latter expression, $(U_B/x_B)/(R/c)$ can be interpreted as the production rate of virtual magnetic photons.

For the first order Compton scattering emissivity we have

$$\varepsilon_c(x_c) = \frac{3}{4}\left(\frac{4}{3}\right)^{\alpha} \frac{\tau_c}{2}\, \ln\Lambda\; \varepsilon_s(x_c) \qquad 1.16$$

where Λ is function of x_c near the extremes of the possible values of x_c, and is constant and equal to $(\gamma_{max}/\gamma_t)^2$ otherwise. Here γ_t is the Lorentz factor of electrons radiating at the selfabsorption frequency x_t, and is given

by (Zdziarski 1986, Ghisellini 1986)

$$\gamma_t \cong \frac{3}{2}\left(\frac{3}{32}\,\frac{\tau_c}{\alpha_f x_B}\right)^{1/(5+2\alpha)} \qquad 1.17$$

where α_f is the fine structure constant, while $x_t=(4/3)\gamma_t^2 x_B$ is

$$x_t \cong \left(\frac{27\sqrt{3}\,3^{\alpha}}{32\,\alpha_f}\,\tau_c\, x_B^{\alpha+3/2}\right)^{2/(5+2\alpha)} \qquad 1.18$$

So, in this simple theory, the synchrotron and the first order Compton spectra have the same slope and this allows to predict X-ray spectral shapes in sources where only the radio and/or the IR-optical flux is observed.

Unfortunately, the hypothesis of a smooth power law in the electron distribution, which is responsible for the same spectral index for synchrotron and IC spectra, is, in general, not self consistent, as will be shown in the next chapter. However, the model in the form described above has been widely applied in the past deriving a number of results which I will summarize below.

1.4 Diagnostic

Combining eqs. 1.15 and 1.17 we can derive the magnetic field B and the relativistic electron density K (or τ_c) as functions of the observable quantities x_t, $F(x_t)$, and the angular size Θ of the source. Although this procedure is widely used, there is no general agreement on the numerical factors relating the magnetic field with the observable quantities. This is because of different definitions of x_t (which can correspond to the peak in the synchrotron spectrum or the energy of unit absorption optical depth), and different geometries used (sphere or slab). See Urry (1984) for an exhaustive analysis and discussion of this problem.

1.5 Predictions

a) Beaming

Knowing the electron density and the magnetic field from the synchrotron spectrum, we can compute the expected IC flux. If the source has been observed in X-rays, where presumably the IC emission contributes, we can compare the predicted with the observed flux. If we make the hypothesis that the source is moving relativistically at an angle φ from the line of sigth, the ratio of the predicted to the observed flux is a measure of the Doppler factor δ defined as

$$\delta = \left[\Gamma - (\Gamma^2-1)^{1/2}\cos\varphi\right]^{-1} \qquad 1.19$$

where Γ is the Lorentz factor associated with the source velocity. This procedure has been followed by many authors, discussing either specific objects or classes of objects (i.e. BL Lacs, OVVs, superluminal sources) thought to be the best candidates to show relativistic bulk motion (see, e.g. Madejski and Schwartz 1983, Madau, Ghisellini and Persic 1986). Note that δ-values derived from the SSC model are independent from those derived by models of superluminal motion.

b) Variability

An obvious expectation of the homogeneous SSC model is that variability in different bands should be related, both in amplitude and timescales. Note however that the first order IC flux depends on the square of the electron density, thus allowing bigger variability in the X-rays (if IC) than in the radio to optical (if synchrotron) range.

c) The L_x-L_o relation

The IC flux should increase more than the synchrotron one for increasing τ_c, while both depend on the same power

of B. Thus we expect a correlation between the optical (L_o) and the X-ray (L_x) monochromatic luminosities of the kind $L_x = const.L_o^a$, with a between 1 and 2 (see Tucker 1983 for a more detailed analysis), contrary to observations of various samples of QSOs and BL Lacs (Zamorani et al. 1981, Maraschi et al. 1983), for which a is less than unity. In QSOs, the presence of a presumably thermal component in the optical-UV (the UV bump), increasingly contributing with increasing luminosity, can account for the above correlation, but this explanation is ruled out for BL Lacs, where no bump is observed.

d) Spectral breaks

The tipical spectrum of a BL Lac object is flat ($<\alpha_R> \cong 0$) in the radio, relatively steep in the IR ($<\alpha_{IR}> \cong 1$), and generally breaks between the IR and the UV, where $<\alpha_{UV}> \cong 1.5$ (Ghisellini et al. 1986). While the break at mm frequencies is generally interpreted as the transition between the partially opaque and the completely thin emission, the break at optical frequencies can be interpreted in the framework of inhomogeneous models, as due to emission from different regions of the source (Ghisellini et al. 1985). An other, and more popular, explanation, is to ascribe this break to the radiative losses of the electrons. If a continuous injection starts at time t_o, after a time $t-t_o$ radiation losses will produce a break in the $N(\gamma)$ distribution at an energy γ_b, to be calculated using eq. 1.7. This break will appear in the synchrotron spectrum at $x_b = (4/3)\gamma_b^2 x_B$. Above x_b, the spectrum is steepened by a factor $\Delta\alpha = 0.5$. But as we have seen, the cooling time is severely limited by the IC losses even for electrons with $\gamma = 1$, and in compact sources the break should move below the selfabsorption frequency after few hours (if not minutes) after the beginning of the injection. However, both suggestions do not explain why the break preferentially is at optically frequencies.

e) Spectral indices

The simple SSC model requires the same spectral index both for synchrotron and IC radiation. In steady state, this index can never be smaller than 0.5, corresponding to s<1 (Rees 1967, cfr eq. 1.11). Flatter spectra must be due to inhomogeneous sources by superposition of emissions from different regions. Alternatively, they are possible for weakly magnetized sources ($U_B << U_r$) in which the IC cooling, although dominant, is limited by the prescription $x\gamma < 3/4$ (see Rees 1967 and next chapter).

1.6 Prescriptions

As early as 1966, Hoyle, Burbidge and Sargent pointed out that compact sources should be characterized by a ratio $U_B/U_r^s > 1$, where U_r^s is the synchrotron energy density, otherwise they would catastrophically cool by the Compton process. This is known as "the Compton limit" or "Compton catastrophe". This limit corresponds to a brightness temperature $T_b < 10^{12}$ °K, where $T_b = I(\nu_t)c^2/\nu_t^2/(2k)$ (Kellerman and P.Toth 1969). When $U_r^s > U_B$, the first order IC luminosity is larger than the synchrotron one by the factor U_r^s/U_b, the second order IC is larger than the first by the same factor, and so on, originating the "catastrophe". But as Rees (1967) pointed out, no more than a few orders IC can be in the Thomson regime, and emission in the Klein Nishina regime is greatly reduced, halting the runaway of emitted energy.

Even if U_B can be smaller than U_r, the maximum brightness temperature is naturally constrained in a little range. Using eqs. 1.15 and 1.18, and since $I_\nu = \varepsilon_\nu R$

$$T_b \cong 1.74 \times 10^{10} (4/9)^{\alpha} (5.74 \times 10^{14} \tau_c/B)^{1/(5+2\alpha)} \qquad 1.20$$

For $\tau_c/B = 10^{-3}$, T_b ranges from 10^{12} to 3.5×10^{11} °K as α

increases from 0.5 to 1. Thus, the fact that most radio sources obey the limit $T_b < 10^{12}$ °K, does not imply the constraint $U_B > U_r^s$, but simply reflects the narrow range possible for T_b.

It can be concluded that the usual prescription $U_B > U_r^s$ has no special meaning, and apparent violations of this inequality are not evidences of relativistic beaming (which would increase the observed U_r). On the other hand, beaming can be responsible for brightness temperatures largely different from those in the narrow range of eq. 1.20.

2. The SSC model revisited

In this chapter I will relax some of the simplifying assumptions made in the standard SSC model, namely I will take into account the effects of synchrotron selfabsorption and constrain the IC cooling to be effective only when $\gamma x < 3/4$. As already noted before, this corresponds to neglecting the cooling in the Klein Nishina regime. This is reasonable, as the IC emissivity in the Klein Nishina regime carries little power compared to that in the Thomson regime, due to the decline of the cross section with energy. Both these effects have been noted and stressed as early as 1967 by Rees, but only very recently they have been discussed again (Zdziarski and Lightman 1985, Zdziarski 1986), while a complete discussion of their effects on the spectrum is still lacking. Since the case of steep injection requires a different treatment, it is discussed separately in the second part of the chapter, where some recent results obtained by Zdziarski and Lamb (1986) in the case of a pure Compton model are extended to the SSC model.

2.1 The continuity equation

It is well known that the selfabsorbed synchrotron spectrum emitted by a power law distribution of electrons is proportional to $\nu^{2.5}$. Thus electrons with $\gamma < \gamma_t$ practically do not loose energy by the synchrotron process, but only via IC scatterings. On the other hand, we make the assumption that electrons of a given γ can scatter only photons with $x < 3/(4\gamma)$. Thus these electrons Compton cool on only a fraction of the total radiation energy density. Taking into account both effects, the continuity equation will be rewritten as

$$N(\gamma) = \frac{3mc}{4\sigma_T}\,\gamma^{-2}\,\frac{\int_{\gamma}^{\gamma_{max}} Q(\gamma')\,d\gamma'}{U_B\,H(\gamma-\gamma_t)+\int_{x_t}^{max(x_t,\,3/4\gamma)} U_r(x)\,dx} \qquad 2.1$$

where H is a step function.

Likely enough, the selfabsorption effect is effective when $U_B > U_r$, while the "Klein Nishina dimming" is important when the opposite is true. Thus we can guess solutions of eq. 2.1 in the two limiting cases, while the general solution has to be found numerically.

2.2 The "X-ray excess"

Consider the case $U_B > U_r$ and suppose that the bulk of U_r is at energies smaller than $1/\gamma_{max}$. For power law injection $Q(\gamma) = A\gamma^{-s}$

$$N(\gamma) = \frac{3mc}{4\sigma_T}\,\frac{\gamma^{-2}}{s-1}\,\frac{A\,\gamma^{1-s}}{U_B\,H(\gamma-\gamma_t)+U_r} \qquad 2.2$$

so that

$$N(\gamma) = \frac{3mc}{4\sigma_T}\,\frac{A}{s-1}\,\frac{\gamma^{-(s+1)}}{U_r}\;; \qquad \gamma<\gamma_t \qquad 2.3$$

$$N(\gamma) = \frac{3mc}{4\sigma_T}\,\frac{A}{s-1}\,\frac{\gamma^{-(s+1)}}{U_r+U_B}\;; \qquad \gamma>\gamma_t \qquad 2.4$$

The $N(\gamma)$ distribution has a discontinuity at γ_t, while retaining the same slope on both sides of γ_t. The "jump" between $\gamma^- = \gamma_t - \varepsilon$ and $\gamma^+ = \gamma_t + \varepsilon$ is

$$(N(\gamma^-)-N(\gamma^+))/N(\gamma^+) = U_B/U_r \qquad 2.5$$

Obviously, no jump can be obtained in the synchrotron spectrum, but this can be observed in the IC one. We can easily compute the first order IC emissivity and compare it to that derived previously. In fact the "new" emissivity will be equal to the "old" one at high energies, where electrons with $\gamma < \gamma_t$ do not contribute, while for low photon energies

we have an extra contribution described by the term enclosed in the square parentheses in the following equation

$$\varepsilon_c(x_c) = \frac{3}{4}\left(\frac{4}{3}\right)^{\alpha}\frac{\tau_c}{2}\,\varepsilon_s(x_c)\,\ln\Lambda\left[1+\frac{U_B\,\ln\Lambda'}{U_r\,\ln\Lambda}\right] \qquad 2.6$$

Care must be taken for the possible values of $\Lambda=x_2/x_1$ and $\Lambda'=x_2'/x_1'$. The energies x_2 and x_1 (and the corresponding primed quantities) are the extremes of the energies of synchrotron photons that can contribute to a given x_c. Their evaluation is tedious, but straightforward. As fig. 1 illustrates, it is convenient to define four characteristic energies

$$\begin{aligned} x_{c1} &= (4/3)x_t \\ x_{c2} &= (4/3)\min(x_{smax},\ x_t\gamma_{max}^2) \\ x_{c3} &= (4/3)\max(x_{smax},\ x_t\gamma_{max}^2) \\ x_{c4} &= \min\left((4/3)\gamma_{max}^2 x_{smax},\ \gamma_{max}\right) \end{aligned} \qquad 2.7$$

We can define also the corresponding primed energies, replacing γ_{max} with γ_t. Thus we have

$$\begin{aligned} &x_{c2}\geq x_c\geq x_{c1} && \Lambda = x_c/x_{c1} \\ &x_{c3}\geq x_c\geq x_{c2} && \Lambda = \min(3x_c/4,\ x_{smax})/\max(x_t,\ 3x_c/(4\gamma_{max})) \\ &x_{c4}\geq x_c\geq x_{c3} && \Lambda = \min(x_{c4}/x_c,\ (\gamma_{max}/\gamma_t)^2) \end{aligned} \qquad 2.8$$

and the same for Λ', with γ_t replacing γ_{max}. For $x_c>x_{c4}'$, $\ln\Lambda'=0$.

It is interesting to derive the spectral index α_x of the IC spectrum and compare it to the canonical index $\alpha_o=s/2$ of the standard SSC model. We have

$$\begin{aligned} \alpha_x &= -\frac{d}{d\ln x}\ln\left[x^{-\alpha_o}\ln\Lambda\left(1+\frac{U_B\ln\Lambda'}{U_r\ln\Lambda}\right)\right] \\ &= \alpha_o - \frac{x}{\ln\Lambda+\frac{U_B}{U_r}\ln\Lambda'}\left[\frac{1}{\Lambda}\frac{d\Lambda}{dx}+\frac{U_B}{U_r}\frac{1}{\Lambda'}\frac{d\Lambda'}{dx}\right] \end{aligned} \qquad 2.9$$

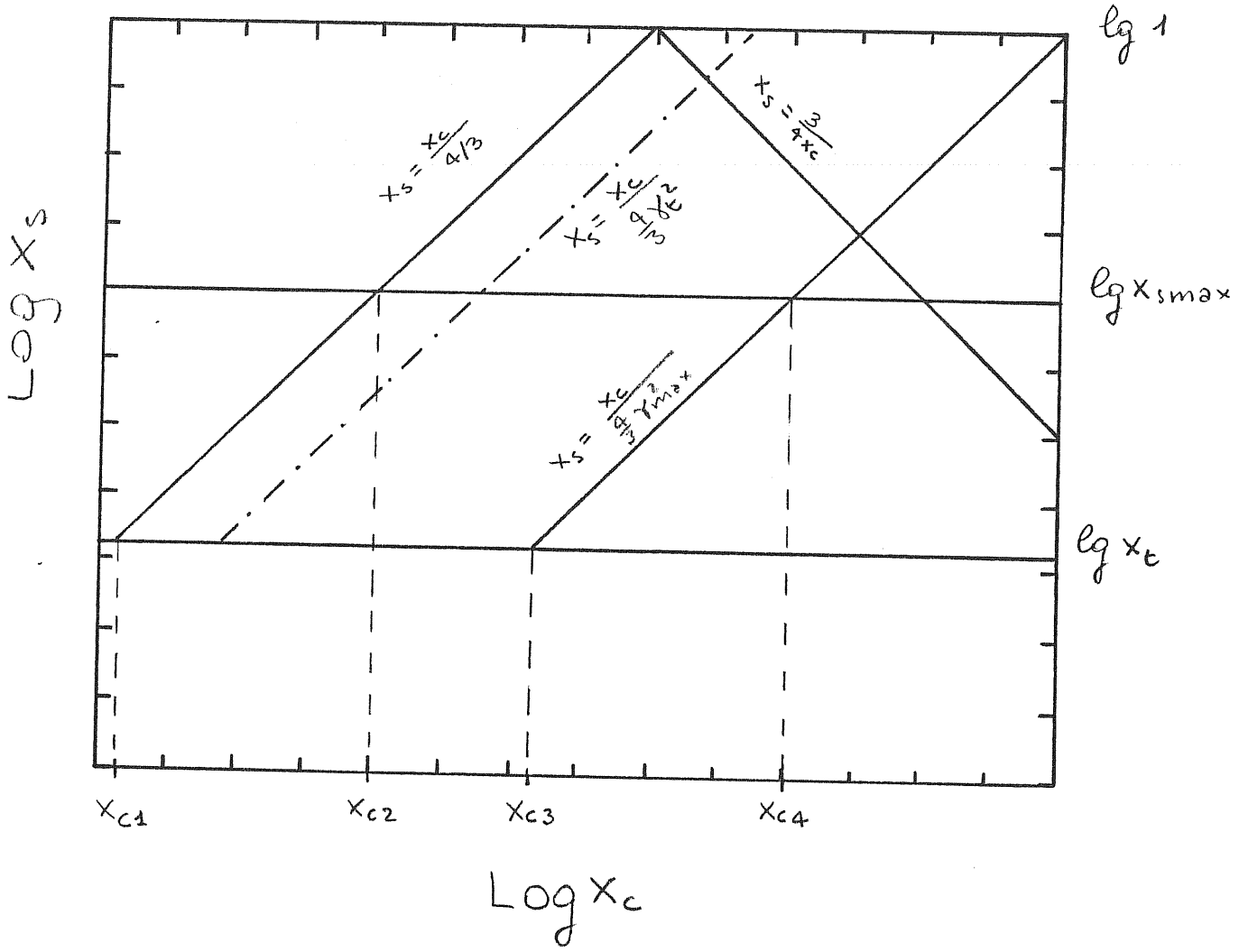

Fig. 1 Schematic diagram for computing the Compton characteristic energies. For a given x_c, only a fraction of incident photons is available.

In Fig. 2 a self consistent spectrum is shown, for $L=10^{45}$ erg/s, $R=10^{15}$ cm, $B=10^{3}$ G and assuming a monoenergetic injection at $\gamma_{max}=10^{3}$. The dashed lined is the spectrum calculated without the selfabsorption effect. For this choice of parameters $U_B/U_r=6.7$. As can be seen, the X-ray spectrum ($x=10^{-3}$ corresponds to 0.5 keV) is steeper than the synchrotron one. In the interesting range 0.5-5 keV, the average spectral index is 0.83. Note that above 30 keV the spectrum flattens, since at these energies only electrons above γ_t contribute, and the usual emissivity (eq. 1.16) can be used.

It must be noted that this "extra emission" increases the values of the beaming factor δ derived in the framework of SSC models neglecting the selfabsorption effect. However, the weak dependence of δ from the X-ray flux (Madau et al. 1986), makes this difference negligible.

2.3 The "Klein Nishina dimming"

For $U_r>U_B$, Compton cooling is dominant and we have to evaluate the integral

$$U_r(\gamma) = \int_{x_t}^{3/(4\gamma)} U_r(x)dx \qquad 2.10$$

For illustrative purposes, suppose that $U_r(x)$ is a smooth power law: $U_r(x)=Ux^{-q}$. Thus the integral will not depend on γ for $q>1$, since in this case the bulk of the energy density is concentrated near x_t. Consequently, if $x_t<3/(4\gamma_{max})$, all electrons Compton cool in the Thomson regime. On the other hand, for $q<1$, we have

$$U_r(\gamma) \div \gamma^{q-1} \qquad 2.11$$

Thus, neglecting U_B, eq. 2.1 yields

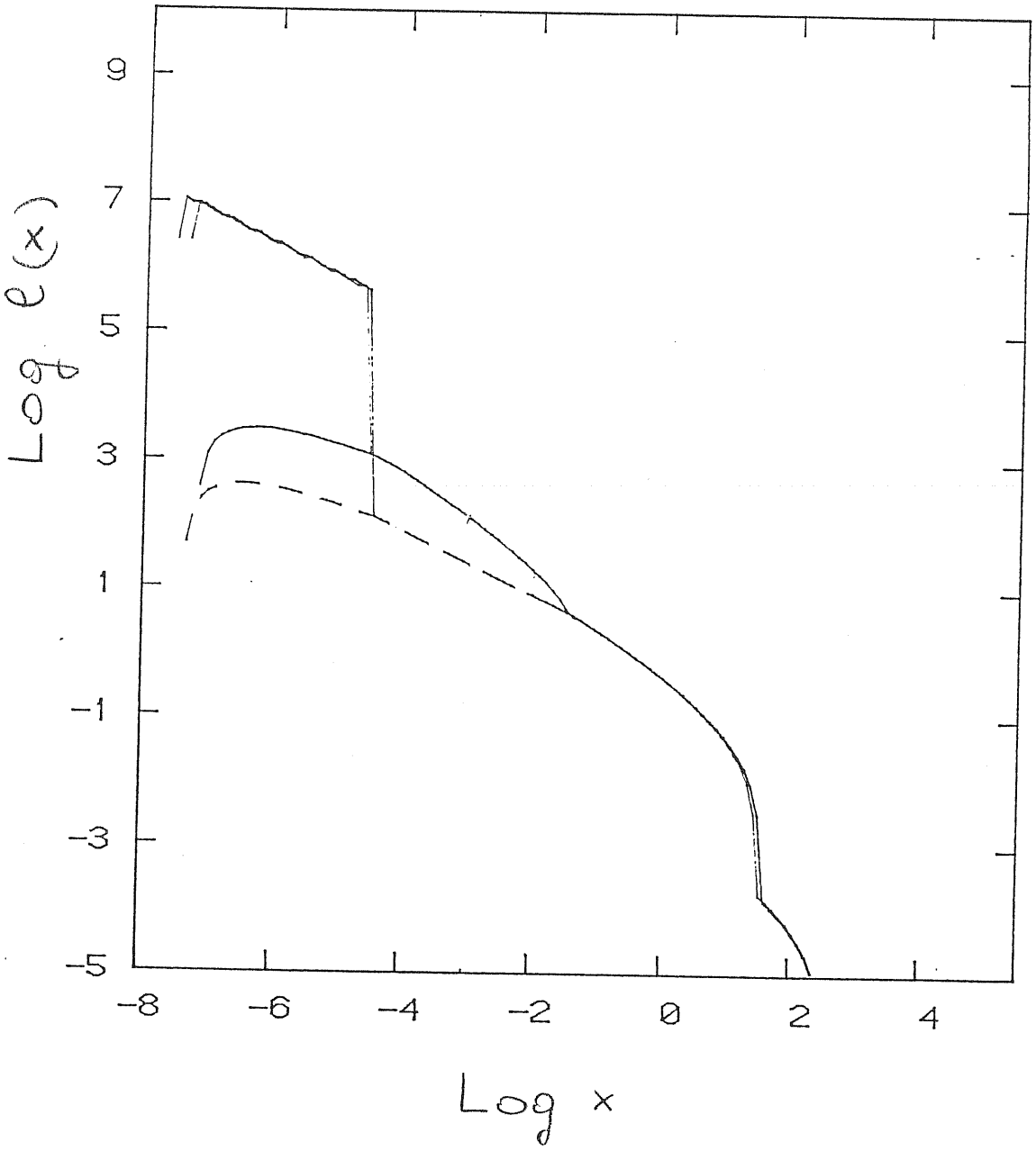

Fig. 2 SSC spectra computed with (solid line) and without (dashed line) selfabsorption effects. The input parameters are: $R=10^{15}$cm, $L=10^{45}$erg/s, $B=10^{3}$G, corresponding to $U_B/U_r=6.7$. A monoenergetic injection at $\gamma_{max}=10^{3}$ is assumed.

$$N(\gamma) \div \gamma^{-(s+q)} \quad \text{for } s>1$$
$$N(\gamma) \div \gamma^{-(1+q)} \quad \text{for } s<1 \qquad 2.12$$

From the relation $q=(p-1)/2$, where p is the slope of $N(\gamma)$, we have

$$q = s-1 \quad \text{for } 2>s>1$$
$$q = 0 \quad \text{for } s<1 \qquad 2.13$$

Comparing these slopes with those derived for complete Thomson cooling ($q=s/2$ for $s>1$ and $q=0.5$ for $s<1$), we see that the spectrum is flatter, with q ranging from 0 to 1.

It is important to stress that this derivation is only qualitative, since we neglected synchrotron cooling, which always affects all electrons, and in particular those that practically cannot Compton cool, due to their large energy. However, this solution is exact in models, different from SSC, where the radiation energy density is dominant and external, namely, not produced by the electrons we are considering. In this case $N(\gamma) \div \gamma^{-(s+q)}$ and there is no relation between s and q.

In general, for $U_B<U_r$ and $s<2$, the SSC spectrum will be flatter than that derived in the usual way, possibly yielding spectral indices α smaller than 0.5. As higher energy electrons loose less energy than low energy ones, the distribution $N(\gamma)$ can be concave, and consequently also the synchrotron spectrum should be flatter at higher energies.

In Fig. 3 an example of self consistent, numerically computed SSC spectrum is shown, for $L=10^{45}$ erg/s, $R=10^{15}$ cm, B=100 G, and a monoenergetic injection with $\gamma_{max}=10^4$. Note that the synchrotron spectrum flattens at high energies. The second order Compton luminosity is also shown (dashed line).

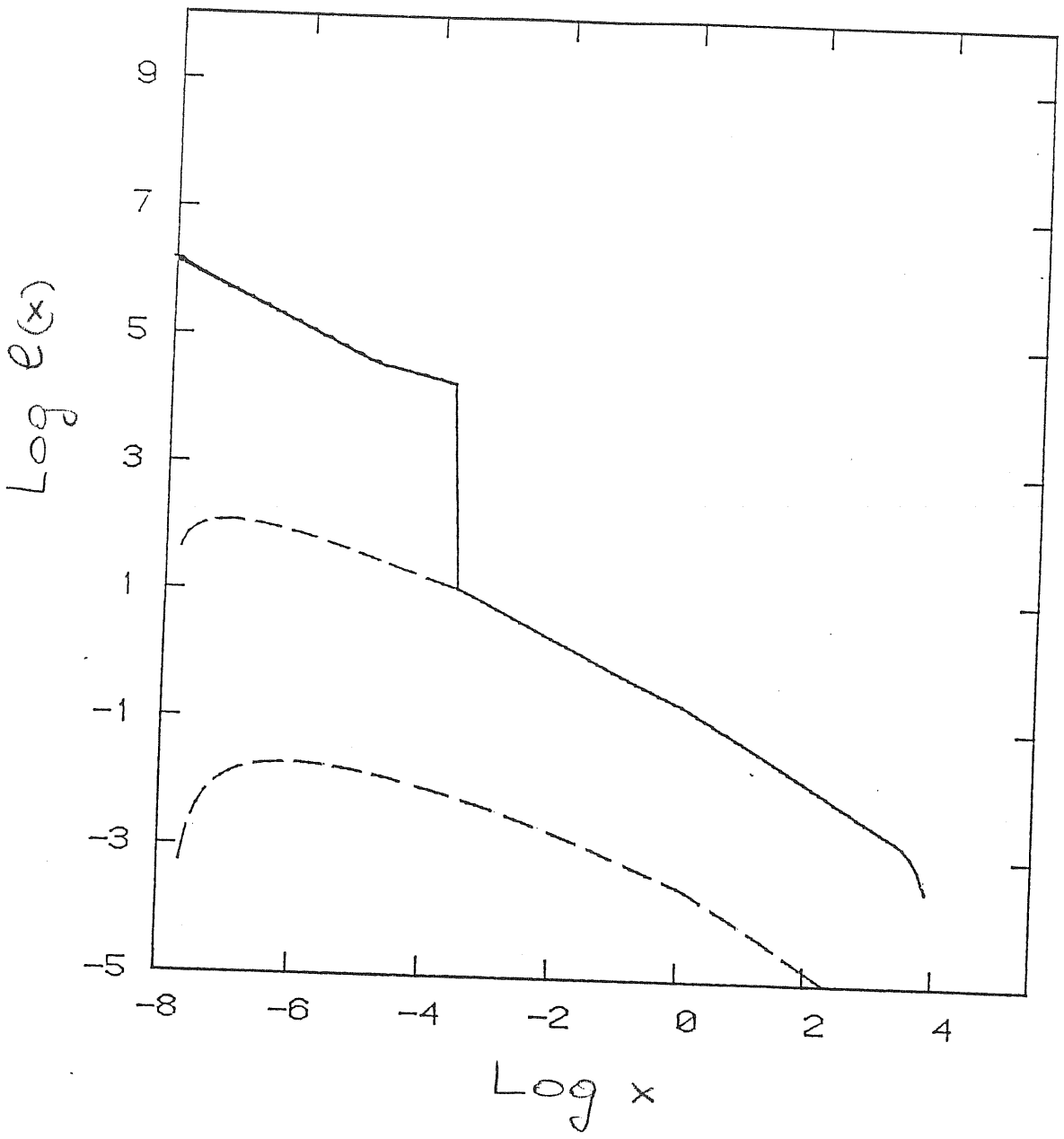

Fig. 3 SSC spectrum for $L=10^{45}$ erg/s, $R=10^{15}$ cm, B=100 G, and mono-energetic injection at $\gamma_{max}=10^{4}$. For these parameters, $U_r/U_B=15$. The flattening at high synchrotron energies is due to the Klein Nishina dimming. The lower dashed line is the 2^{nd} order Compton spectrum.

2.4 The case of steep injection

Consider to inject a power law of relativistic electrons, $Q(\gamma)=A\gamma^{-s}$, with $s>2$. In this case most of the power is injected at low energies, where the synchrotron emission is inhibited by selfabsorption. Consequently, the Compton process is the dominant cooling mechanism, even for $U_B>>U_r$, provided that reacceleration is negligible, and that the cooling timescale is shorter than those of other competing processes, for all relativistic electron energies.

If the injected particles are electrons escaping from the source in a timescale t_{esc} with velocity $c\beta_{esc}$, the condition $t_{cool}<t_{esc}$ (for any γ) reads

$$\ell > \frac{4\pi}{3}\,\frac{\beta_{esc}}{1+\tau_T} \qquad 2.14$$

where ℓ is the dimensionless compactness parameter

$$\ell = \frac{L\,\sigma_T}{R\,mc^3} \qquad 2.15$$

and τ_T is the Thomson optical depth of the cool electrons. It can be estimated balancing the injection and the escape rate

$$\tau_T \cong \frac{3}{4\pi}\,\frac{s-2}{s-1}\,\frac{\ell}{\beta_{esc}} \qquad 2.16$$

Combining eqs. 2.14 and 2.16 the minimum value of τ_T is

$$\tau_{T,min} = \frac{1}{2}\left[\left(4\,\frac{s-2}{s-1}+1\right)^{1/2}-1\right] \qquad 2.17$$

which is close to, but smaller than unity. If we want to neglect all the effects associated with cool particles such as downscattering, thermal Comptonization, and photon diffusion, we must require $\tau_T<1$. For $1>\tau_T>\tau_{T,min}$ the possible values of ℓ are limited in a narrow range of the order $4.2\beta_{esc}>\ell>1.5\beta_{esc}$ (for $s=3$).

On the other hand, if the injected particles are pairs, and assuming that they cannot escape, but only annihilate in a timescale t_A, we always have $t_{cool} < t_A$ (see chapter 4 for definition of t_A) since the annihilation cross section is small at high energies. The optical depth of cool pairs can now be derived balancing the pair injection and annihilation rate

$$\tau_T \cong \left(\frac{4}{\pi} \frac{s-2}{s-1} \ell \right)^{1/2} \qquad 2.18$$

and the condition $\tau_T < 1$ yields $\ell < (s-1)/(s-2)(\pi/4) \sim 1$.

If Compton losses were absent, the electrons below γ_t would tend to form a Maxwellian distribution at some relativistic temperature Θ (Rees 1967), through Coulomb collisions. The relaxation t_{ee} time for this process at relativistic temperatures is given by Stepney (1983)

$$t_{ee} = 8\Theta^2/\ln\Lambda \quad ; \quad \Theta >> 1 \qquad 2.18a$$

where $\ln\Lambda$ is the Coulomb logarithm. Comparing t_{ee} with t_{cool} (eq. 1.7) we derive the minimum compactness above which t_{ee} is longer than t_{cool} for any γ

$$\ell > \frac{\pi}{6} \tau_c \ln\Lambda \qquad 2.18b$$

which gives, for $\ln\Lambda = 20$ and $s=3$, $\ell > 1.7$.

For steep injection the ratio of the Compton to the synchrotron luminosity is

$$L_C/L_S = \frac{\int_1^{\gamma_t} \dot{\gamma}_c N(\gamma) d\gamma + \int_{\gamma_t}^{\gamma_{max}} \dot{\gamma}_c N(\gamma) d\gamma}{\int_{\gamma_t}^{\gamma_{max}} \dot{\gamma}_s N(\gamma) d\gamma} \qquad 2.19$$

If $U_B >> U_r$ this expression simplifies into

$$L_c/L_s \cong \frac{\int_1^{\gamma_t} \gamma Q(\gamma) d\gamma}{\int_{\gamma_t}^{\gamma_{max}} \gamma Q(\gamma) d\gamma} = \frac{\gamma_t^{s-2} - 1}{1 - (\gamma_t/\gamma_{max})^{s-2}} \qquad 2.20$$

which is indipendent on the Compton cooling regime (Klein-Nishina or Thomson). For $U_r > U_B$ this ratio will approximately increase by the factor U_r/U_B. Using eq. 1.17 we have

$$\gamma_t^{s-2} \cong \left(\frac{3}{2}\right)^{s-2} \left[\frac{3}{32 \alpha_f} \frac{s-2}{s-1} \frac{U_r}{U_B} \frac{\beta_c}{\beta} \right]^{\frac{s-2}{s+5}} \qquad 2.21$$

so that L_c/L_s increases for steeper injections.

All the power injected below γ_t has to be released through many orders IC scatterings, as can be realized computing the ratio of the first order to the total Compton luminosity

$$L_c^{1st}/L_c = U_r^s/U_r = \gamma_t^{-s+2} << 1 \ , \ (U_B >> U_r) \qquad 2.22$$

The Klein Nishina limit will play a double important role: first, it constraints the number of IC orders that contribute to the overall spectrum to be finite, and, second, it fixes the slope of the γ-ray spectrum, which will be greater than unity, as shown in the following.

To derive the final spectrum analytically, without computing each contribution, I will assume that the overall spectrum is a power law with index α_c from x_o to 1, and with index α_γ from 1 to γ_{max}. I will take x_o as the energy where the synchrotron and the first order IC emissions are equal.

With these assumptions it is easy to realize that $\alpha_c \leq 1$, since for photon conservation the overall IC spectrum cannot be greater than the synchrotron one at energies close to x_t, while the integrated IC luminosity greatly exceeds the synchrotron one.

2.4a Determination of α_γ

The continuity equation gives for the steady density energy distribution, in the case of $\tau_T<1$

$$\sigma_T R N(\gamma) = \frac{s-2}{s-1} \frac{\gamma^{-(s+1)}}{\frac{U_B}{U_r} H(\gamma-\gamma_t) + f(\gamma)} \qquad 2.23$$

where $f(\gamma)$ takes into account the Klein Nishina limit to the cooling and is given by

$$f(\ ) = \begin{cases} \ln\frac{3}{4x_0\gamma} \dfrac{1}{\ln 1/x_0 + (1-\gamma_{max}^{1-\alpha_\gamma})/(\alpha_\gamma-1)}, & \alpha_c = 1 \\ \dfrac{(3/4\gamma)^{1-\alpha_c} - x_0^{1-\alpha_c}}{1-x_0^{1-\alpha_c} + (1-\alpha_c)(1-\gamma_{max}^{1-\alpha_\gamma})/(\alpha_\gamma-1)}, & \alpha_c \neq 1 \end{cases} \qquad 2.24$$

Depending on the ratio U_B/U_r, $N(\gamma)$ can have a very different normalization on the opposite sides of γ_t. Thus it is very important to know if photons of energy $x>1$ result from the scattering of low energy photons by high energy electrons, or vice-versa. The latter case is always favourite if downscattering is absent, as can be seen directly computing the Compton emissivity at energies $x>1$ (Zdziarski 1986)

$$\varepsilon_C(x_C) = \frac{\sigma_T c}{2} \int_{x_1}^{3/4x_c} n(x)\, N(\gamma)\, \gamma\, dx; \quad \gamma = \left(\frac{3x_c}{4x}\right)^{\frac{1}{2}}; \quad x_c \geq 1 \qquad 2.25$$

where $n(x)$ is the monochromatic photon density, $n(x)=x^{-(1+\alpha_c)}$ The limits of the integral are the possible energy range of incident photons. From eq. 2.23 with $\alpha_c<1$, $N(\gamma) \div \gamma^{-(s+q)}$, where q can be α_c or 1, depending on γ and on the ratio U_B/U_r. Then the integrand of eq. 2.25 is

$$n(x)N(\gamma)\gamma \div x^{\frac{s+q-2\alpha_c-3}{2}} \qquad 2.26$$

Since $(s+q-2\alpha_c-3)/2>-1$ in any case, the upper limit of the integral is important, meaning that γ-rays are mainly produced by low energy electrons scattering high energy photons.

Furthermore, we can now calculate the γ-ray slope α_γ, considering that only electrons with $\gamma<\gamma_t$ contribute. In this case $q=\alpha_c$, and eq. 2.25 gives

$$\varepsilon_c(x_c) \div x_c^{-(s-1)} \; ; \qquad x_c \geq 1 \qquad 2.27$$

independently of α_c. Thus a sharp break is expected to occur at x=1, and since s>2, the γ-ray luminosity will be only a small fraction of the total. Note that this break has nothing to do with the break caused by γ-γ absorption and pair production, which in some case can seem very similar to the one discussed here (see next chapters). With the particular slope of the γ-ray spectrum of eq. 2.27, it is also very easy to qualitatively account for pair production. At most, in fact, all γ-ray photon can be converted into pairs colliding with X-ray photons. Since $n(x)\div x^{-s}$ for x>1, and since the energy of the created particles are approximately half of the γ-ray photon, the pair production rate $P(\gamma)\div\gamma^{-s}$. Then, primary injected particles and injected pairs have the same slope, leaving unaltered the shape of the spectrum below x=1. Note, however, that we are neglecting the influence of cool electrons (or pairs) that will introduce other effects, as will be shown below.

2.4b Determination of α_c

At energies close to x_t, only the synchrotron and the first order Compton emission are important, and they are equal at the energy x_o

$$x_o = (4/3)x_t \exp\left[\frac{1}{2}\left(\frac{3}{4}\right)^{\frac{s}{2}-1}\frac{s-1}{s-2}\right] \qquad 2.28$$

At this energy the total emission is approximately twice the synchrotron one. Above x=1, the spectrum steepens with $\alpha_\gamma=s-1$, and luminosity balance ($L_{in}=L_{out}$) requires

$$L = 2L_s(x_o)\left\{\int_{x_o}^{1}\left(\frac{x_o}{x}\right)^{\alpha_c}dx + \frac{1}{2}\int_{x_t}^{x_o}\left(\frac{x_o}{x_t}\right)^{\frac{s}{2}}dx + x_o^{\alpha_c}\int_{1}^{\gamma_{max}} x^{-\alpha_\gamma}\,dx\right\} \qquad 2.29$$

The monoenergetic synchrotron luminosity can be related to the total synchrotron one, and eq. 2.29 becomes

$$x_o^{\alpha_c - 1} = \frac{\frac{L_c}{L_s}\left(\frac{x_o}{x_t}\right)^{\frac{s}{2}-1}\left[1-\left(\frac{\gamma_t}{\gamma_{max}}\right)^{s-2}\right] + 1 - \left(\frac{x_o}{x_t}\right)^{\frac{s}{2}-1}\left(\frac{\gamma_t}{\gamma_{max}}\right)^{s-2}}{1 + (s-2) f(\alpha_c)}$$

$$f(\alpha_c) = \begin{cases} \ln(1/x_o), & \alpha_c = 1 \\ \frac{1 - x_o^{1-\alpha_c}}{1-\alpha_c}, & \alpha_c \neq 1 \end{cases} \qquad 2.30$$

in the case $U_B >> U_r$ and $\gamma_{max} >> \gamma_t$, eq. 2.30 simplifies into

$$x_o^{\alpha_c - 1} = \frac{(x_o/x_t)^{\frac{s}{2}-1}(\gamma_t^{s-2} - 1)}{1 + (s-2) f(\alpha_c)} \qquad 2.31$$

2.4c Effects of cool particles

In the case of optical depth τ_T greater than unity, we have to take into account photon diffusion, Comptonization of soft photons by thermal subrelativistic particles, and downscattering of hard photons.

Photon diffusion enhances the photon density by a factor

$$\phi = 1 + \tau_T / a \qquad 2.32$$

where a is of order unity and depends on geometry (=3 for a sphere). The first order Compton emissivity will be increased by a factor ϕ, the second order by a factor ϕ^2, and so on.

Thermal Comptonization will be important between x_t and $x \cong \Theta = kT/mc^2$, while downscattering will steepen the spectrum between $x = 1/\tau_T^2$ and $x=1$ by a factor dependent on the spatial distribution of the photon sources (Sunyaev and Titarchuk 1980). We will assume $\Delta\alpha = 0.5$, appropriate for an uniform distribution.

All these effects can be simply estimated changing our luminosity balance equation and the equation for x_o. Since the first order IC emission is increased by a factor ϕ

$$x_o = (4/3)x_t \exp\left[\frac{s-1}{s-2} \frac{(3/4)^{\frac{s}{2}-1}}{2\phi} \right] \qquad 2.33$$

Neglecting the γ-ray luminosity, the luminosity balance equation is now

$$L \cong 2L_s(x_o)\left\{ \int_{x_o}^{1/\tau_T^2} \left(\frac{x_o}{x}\right)^{\alpha_c} dx + \frac{1}{2}\int_{x_t}^{x_o} \left(\frac{x_o}{x}\right)^{\frac{s}{2}} dx + \int_{1/\tau_T^2}^{1} \frac{1}{\tau_T}\left(\frac{x_o}{x}\right)^{\alpha_c} x^{-1/2}\, dx \right\} \qquad 2.34$$

The derived α_c would in general be flatter than that derived before, since most of the luminosity is now emitted in a restricted range of energies, while the normalization of the spectrum at x_o remains almost constant, due to the opposite effects that Comptonization and increased cooling (reducing $N(\gamma)$) have on the low energy synchrotron emission.

The resulting spectrum will be a broken power law, with slope α_c up to $x=1/\tau_T^2$ and $\alpha_c+1/2$ between $1/\tau_T^2$ and 1. In the latter range the photon number density will be $n(x) \div x^{-2-\alpha_c}$ (Svensson 1986), and eq. 2.26 now reads

$$n(x)N(\gamma)\gamma \div x^{(s+q-5-2\alpha_c)/2} \qquad 2.35$$

the upper limit of the integral will now be important if

$$s > 3+2\alpha_c-q \qquad 2.36$$

where q can be 1 or α_c. This condition is not always satisfied. When it is, the slope of the γ-ray spectrum will be $\alpha_\gamma = s-2$, different from what derived before, but steeper than unity in any case, as s must satisfy eq. 2.36.

If $s<3+2\alpha_c-q$, the γ-rays are produced by low energy photons scattering high energy electrons and the slope is

$$\alpha_\gamma = 1+\alpha_c \; ; \qquad \gamma_{max} >> x \gtrsim 1 \qquad 2.37$$

so that a further steepening of a factor $\Delta\alpha=0.5$ occurs at x=1, with respect to the downscattered spectrum between $1 > x > 1/\tau_T^2$.

2.4d Comparison with numerical results

This approximate, but simple, analytical treatment describes numerical results quite accurately, as can be seen from the fig. 4, 5, 6, 7. All the figures refer to the same luminosity and size, corresponding to $\ell \cong 27$, and value of the injection slope s=3. The spectra in fig. 4 and 5 are computed without cool particle effects for two different values of the magnetic field, corresponding to $U_B/U_r=1.67$ and 107, respectively. The synchrotron and several orders IC spectra are also shown. Labels correspond to spectral index of the total emission. Using eq. 1.18 for x_t and eqs. 2.29 and 2.31, one obtains $\alpha_c \cong 0.89$ for both cases, in excellent agreement with the spectra obtained numerically. Moreover, $\alpha_\gamma \sim 1.9 \sim s-1$, as predicted. Numerical results (not shown here) computed with s=2.5 (all the other parameters being the same) are also in agreement with the analytic results discussed above. In particular, it is confirmed that flatter injections, and thus smaller ratios L_c/L_s, make the spectrum steeper.

Fig. 6 and 7 show spectra calculated including the effects of cool particles, for the same parameters of fig. 4 and 5, respectively. Thermal Comptonization is computed assuming that a monoenergetic radiation transforms in a power law of index (Sunyaev and Titarchuk 1980)

$$\alpha_{th} = \left(\frac{9}{4} + \frac{\pi^2}{3(\tau_T + 2/3)^2\, \Theta} \right)^{1/2} - \frac{3}{2} \qquad 2.38$$

with a cutoff at $x=\Theta$. Compton balance fixes the temperature

$$\Theta \cong \frac{1}{4} \frac{\int_{x_t}^{1} x\, U_r(x)\, dx}{\int_{x_t}^{1} U_r(x)\, dx} \qquad 2.39$$

In this approximate treatment of Comptonization we neglect the exponential tail which should be present in the Comptonized spectrum above $x = \Theta$. The kinks at energies $x \cong \Theta$ in figs. 6 and 7 are due to this approximation. Dashed lines correspond to the spectra of figs. 4 and 5, reported for an easy comparison. Labels correspond to spectral indices of the continuous line.

Note that α_γ is effectively well described by eq. 2.37, and that α_c is flatter than the correspondent case without cool particles.

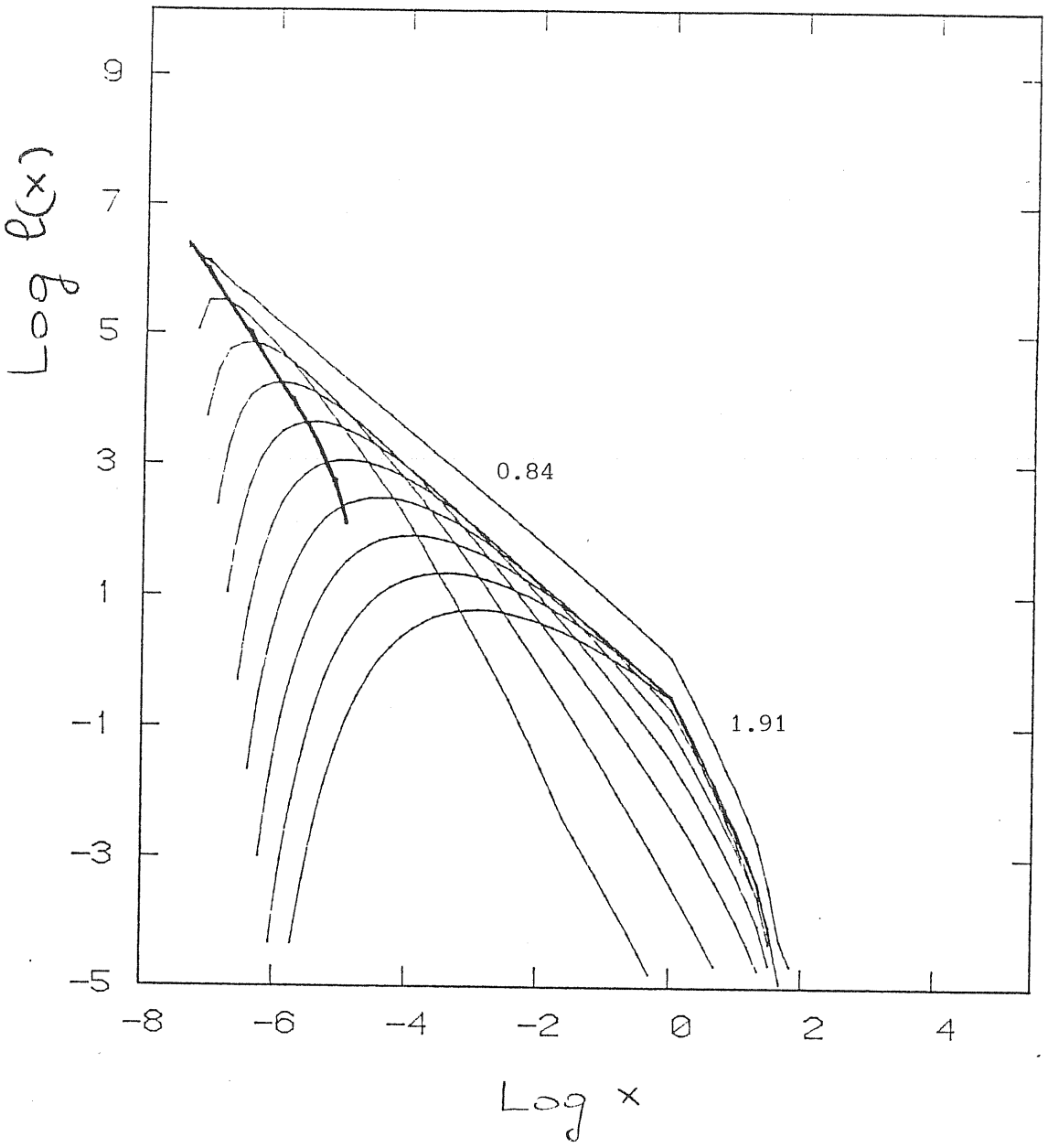

Fig. 4 SSC numerically computed for $L=10^{45}$, $R=10^{15}$cm, B=500 G and power law injection with index s=3, up to $\gamma_{max}=10^{3}$. For these parameters $U_B/U_r \cong 1.67$, and $\ell=27$. Cool particle effects are neglected. Spectral indices in different bands are reported.

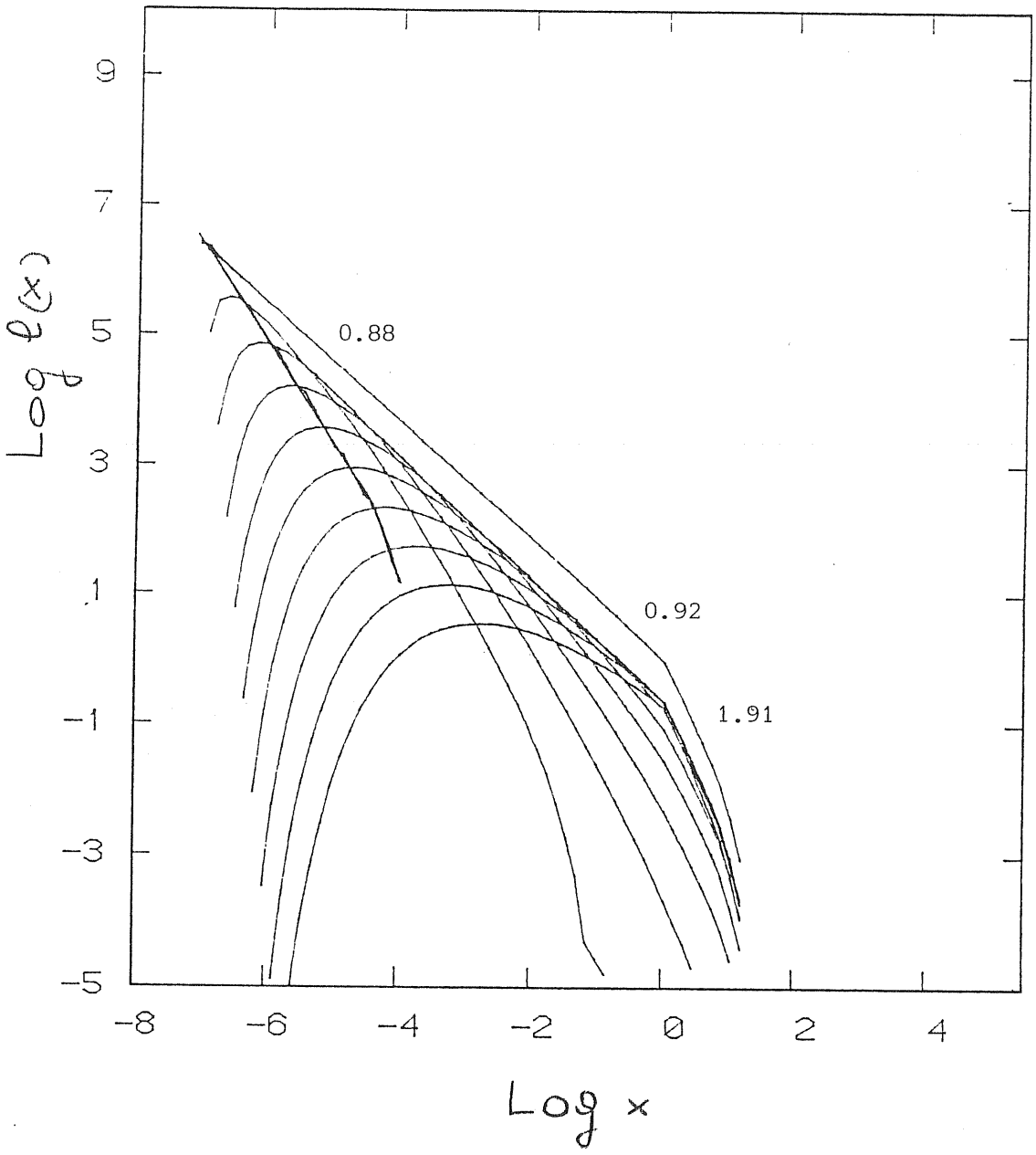

Fig. 5. SSC spectrum numerically computed for the same parameters of Fig. 4, but with $B=4\times10^{3}$G, yielding $U_B/U_r \cong 107$. Cool particle effects are neglected. Spectral indices in different bands are reported.

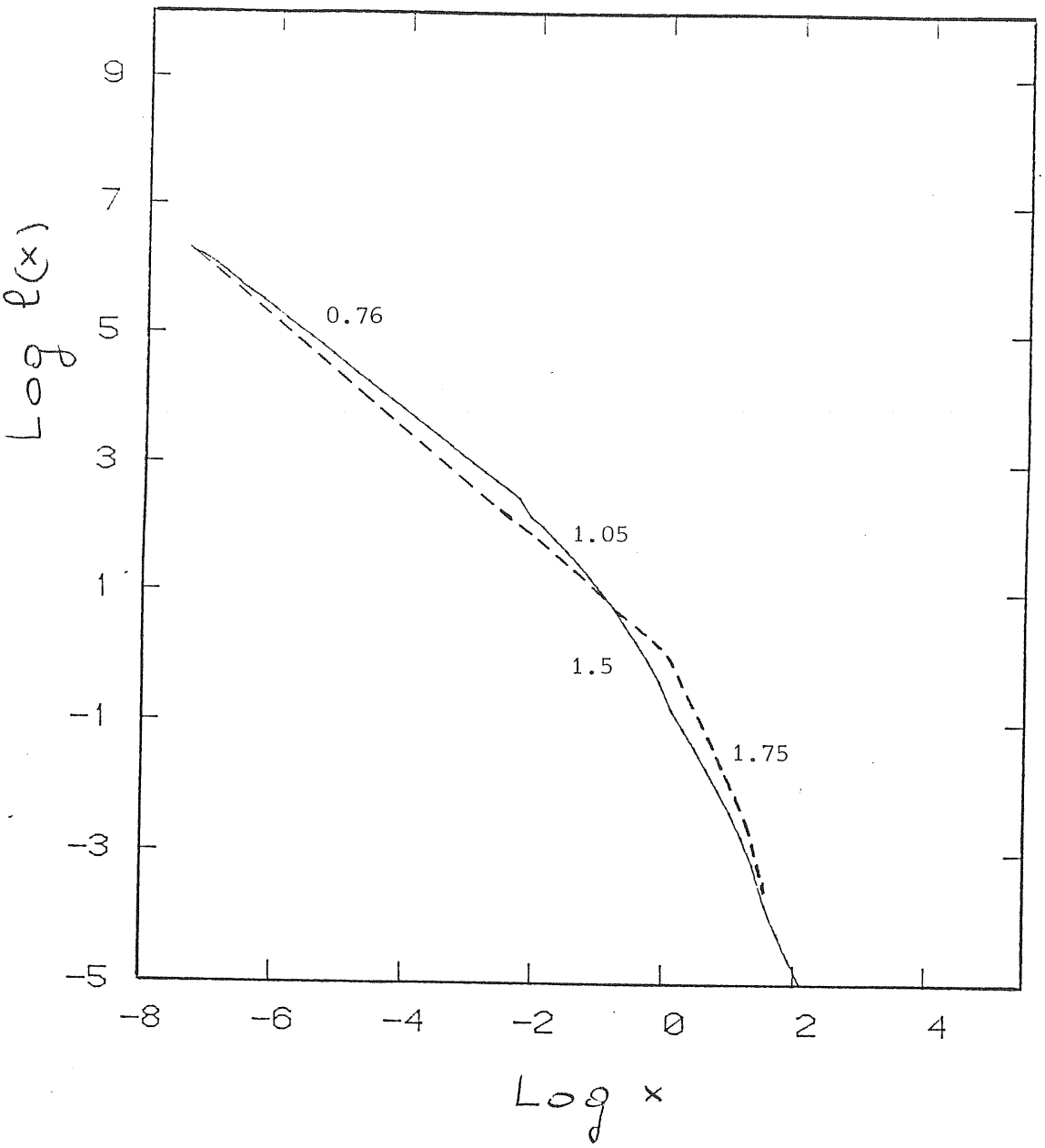

Fig. 6. SSC spectrum numerically computed for the same parameters of Fig. 4, but including cool particles effects. The injected particles are assumed to be pairs. The Thomson optical depth $\tau_T \cong 4.15$, the Compton temperature $\Theta \cong 8.6 \times 10^{-3}$. The overall spectrum of fig. 4 is reported (dashed line) Labels indicate spectral indices in different bands, and refer to the continuous line.

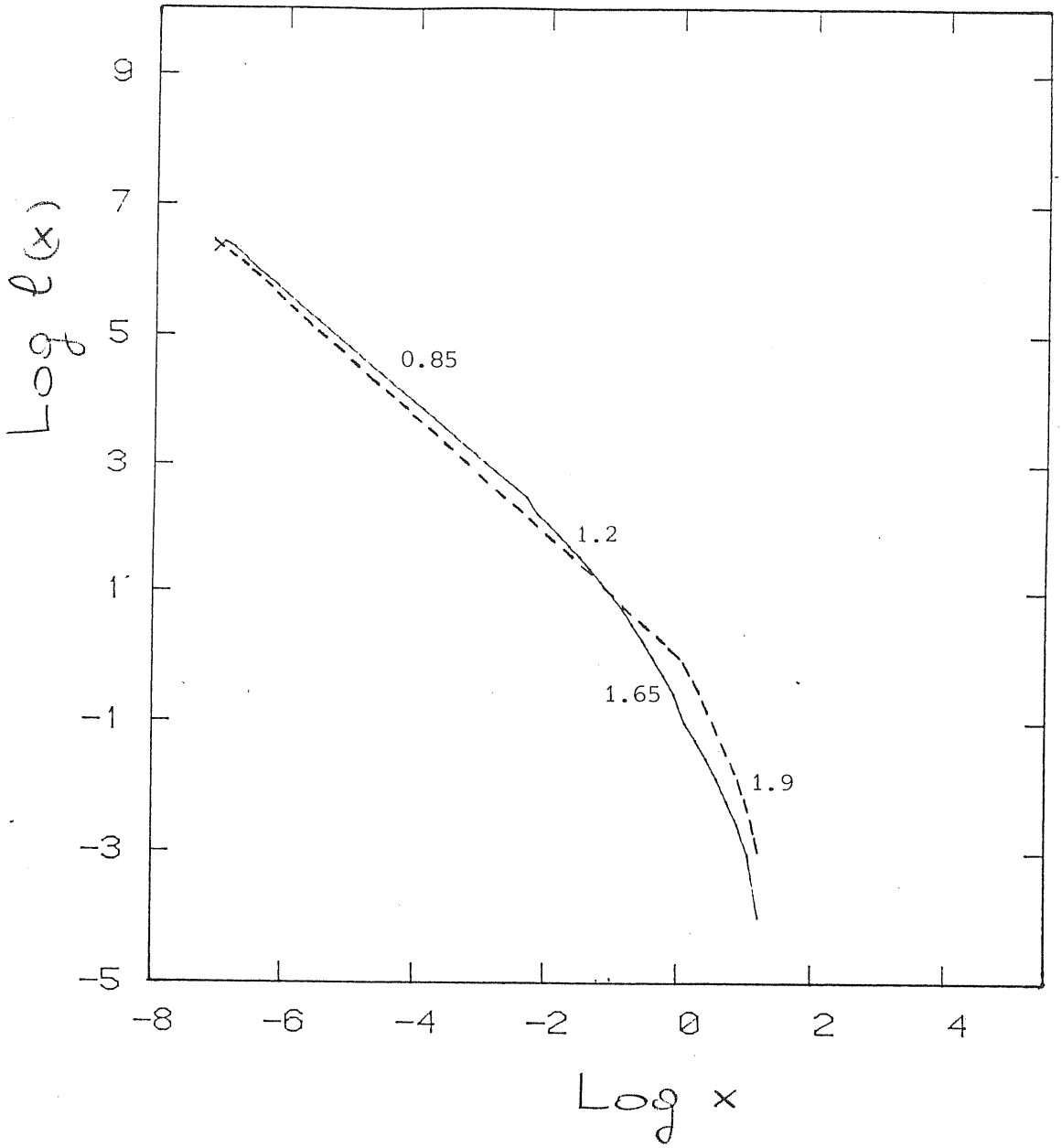

Fig. 7. SSC spectrum numerically computed for the same parameters of Fig. 5, but including cool particle effects. The injected particles are assumed to be pairs. The Thomson optical depth $\tau_T \cong 4.15$, the Compton temperature $\theta \cong 6 \times 10^{-3}$. The overall spectrum of Fig. 5 is reported (dashed line). Labels indicate spectral indices in different bands, and refer to the continuous line.

3. The importance of pair production in non-thermal models

Even if this thesis is mainly concerned with the SSC model, it will be instructive to review some recent results in a simple Compton model, where no magnetic field is considered. These results have been obtained by Fabian (1984), Zdziarsi and Lightman (1985), Fabian et al. (1986), and Svensson (1986a, b).

Due to high photon densities in compact sources, the main process yielding pairs is photon-photon collision, which has a threshold x_{th}

$$x_{th} = \frac{2}{x_1 (1 - \cos\theta)} \qquad 3.1$$

where θ is the angle between the two photons of energies x_{th} and x_1. Due to the peak of the cross section around $2x_{th}$, collisions preferentially take place between photons of reciprocal energies x and 1/x as long as a constant or decreasing (with energy) distribution of photons is involved. Since the peak value of the cross section approaches the Thomson cross section, it is convenient to define a dimensionless luminosity ℓ in this way

$$\ell = \frac{L}{R} \frac{\sigma_T}{mc^3} \qquad 3.2$$

which is a measure of the optical depth for photon-photon interactions

$$\tau_{\gamma\gamma}(x) = \int_{x_{th}}^{x_{max}} \sigma_{\gamma\gamma}(x, x') R \, n_\gamma(x') dx' \qquad 3.3$$

where $n_\gamma(x)$ is the photon number density of energy x. A very accurate expression for $\tau_{\gamma\gamma}(x)$ has been derived by Svensson (1986b) in the case of power law distributions $n(x) \div x^{-\alpha-1}$

$$\tau_{\gamma\gamma}(x) = \eta(\alpha) \sigma_T R n(1/x)/x \qquad 3.4$$

$$\eta(\alpha) \cong (7/6)(1+\alpha)^{-5/3}(2+\alpha)^{-1} \qquad 3.5$$

where α must be evaluated at the energy x^{-1}. From eqs. 3.2 and 3.4 one can see that if the bulk of the luminosity is emitted at MeV energies (x=1), we have, apart from factors of order unity

$$\ell \sim 4\pi \tau_{\gamma\gamma}(1) \qquad 3.6$$

So that γ-ray absorption and pair production are important for $\ell \geq 4\pi$ in hard X-rays, or for the compactness parameter $L_X/R > 4.6\times10^{29}$ erg s^{-1} cm^{-1}. However, pairs start to affect the emitted spectrum if $\tau_{\gamma\gamma}(x_{max}) \gtrsim 1$, while pair production saturates when $\tau_{\gamma\gamma}(1) \gtrsim 1$.

Assuming that the source is powered by accretion onto a black hole, we can write ℓ in terms of the Eddington luminosity L_E and the Schwarzshild radius R_s. For non rotating black holes

$$\ell = 2\pi/3(m_p/m_e)(L/L_E)3R_s/R \qquad 3.7$$

and this gives the upper limit $\ell < \ell_E \sim 4000$. Note that if the source is pair dominated, its Eddington luminosity is a factor m_p/m_e lower than the usual one, as pairs are lighter than protons. Combining eq. 3.7 with 3.6, we have that pairs are important for sources emitting more than 1% of their Eddington luminosity in hard X-rays, which seems to be a fairly tipical value for AGNs (i.e. Wandel and Mushotzky 1986), assuming no relativistic beaming. If this is present, and calculating $\tau_{\gamma\gamma}$ from the observed luminosity and the observed variability timescale

$$\tau'_{\gamma\gamma}(x') = \tau'_{\gamma\gamma}(x/\delta) = \tau_{\gamma\gamma}(x')\delta^{4+\alpha} \qquad 3.8$$

where primed quantities are in the observer frame and δ is the Doppler factor defined by eq. 1.19. If the beaming of

the radiation is not due to relativistic motion, but only to collimation (by e.g. a thich disk funnel) in the observer direction, than $\tau'_{\gamma\gamma}(x') \simeq (4\pi/\Omega)\,\tau_{\gamma\gamma}(x')$, where Ω is the solid angle of the beam.

In the remaining of this section, we will consider the case in which the injected electrons only make inverse Compton scatterings on a fixed and independent soft photon source, without making synchrotron photons. We will call the soft photon energy density as U_{ext}. If U_{ext} is greater than the energy density produced by the electrons, we can neglect the higher order IC scatterings, as was the case for $U_B > U_r$ and flat injection in the SSC model. Furthermore in this case the IC spectrum becomes independent of U_{ext}: increasing U_{ext} we increase the number of the photon that can be scattered, but at the same time we decrease the number density of the electrons (they cool more) by the same factor (Zdziarski and Lightman 1985). Thus we do not expect, in this case, correlated variability between the soft photon emission and the Comptonized spectrum.

Pairs will be produced by γ-ray photons colliding with X-ray photons: they will share the available energy

$$\gamma_- + \gamma_+ = x + 1/x \qquad 3.9$$

and it turns out that for power law spectra $\ell(x) \div x^{-\alpha}$ it is a good approximation to assume

$$\gamma_{\pm} \simeq x/2 \qquad 3.10$$

as long as $\alpha > 0.5$ (Bonometto and Rees 1971, Svensson 1986b). The created pairs will radiate and cool, and they can be thougth as an extra injection $P(\gamma)$, besides the injection of primary particles $Q_o(\gamma)$. Eventually, the energy of the pairs is large enough to Compton scatter soft photons above threshold for pair production, thus yielding a new

generation of pairs, and so on.

The non linearity of the process does not allow a general analytic solution for the emergent spectrum, even if only the first order Compton scattering is considered, because:

i) The pair production rate depends on the photon production rates at the two energies x and 1/x (incident and target photons);

ii) This rates depend on the pair production rate (pairs make photons);

iii) The density of the cool pairs can be large enough to change the photon energy density, through photon diffusion;

iv) Cool pairs will be heated by hard photons undergoing downscattering, and cooled by soft photons by upscattering, thus changing the spectrum both in the soft and high energy bands.

Despite all these complications, a general statement is possible even at this stage: pairs will steepen the primary spectrum. In fact high energy radiation will be absorbed and redistributed towards smaller energies by both the relativistic (1st reprocessing) and cool (2nd reprocessing) pairs.

For power law spectra of index α, $\alpha=1$ is a particular value, because for flatter slopes most of the power is emitted at high energies, and for large compactnesses the reprocessing will be strong, while for steeper spectra the reprocessed power will be only a small fraction of the bolometric luminosity, and the spectrum will not be greatly affected even for large compactnesses.

A very simplified treatment of the problem was first done by Bonometto and Rees (1971) who obtained $\alpha \sim 1$ as the self consistent slope of the spectrum in the case of saturated pair production, this result being confirmed by Kazanas (1984) using a slightly different approach. In both papers cool particles were neglected.

Zdziarki and Lightman (1985) found analytical and semi-analytical solutions for the emergent luminosity when $\tau_{\gamma\gamma}(x)$ is less than unity for all photon energies x. In this case pair production can be handled as a perturbation to the primary injection and the pair plasma does not become optically thick to Thomson scattering. If moreover only one generation of pairs is possible, only the primary particles are emitting above the threshold for pair production. Then the pair production rate will only depend on the density of target photons which is found analytically. In order to have $\tau_{\gamma\gamma}(x_{max}) \lesssim 1$, low compactnesses ℓ must be considered, and thus pair effects are small. Nevertheless, for monoenergetic electron injection (which yields $\alpha = 0.5$ without pairs) the X-ray spectrum steepens with increasing luminosity, reaching slopes of $\alpha \sim 0.7$ for the largest luminosity compatible with the previous assumptions.

The opposite case was considered by Svensson (1986b). When $\tau_{\gamma\gamma}(x) > 1$ for all energies $x > 1$, we can approximate the γ-ray absorption with a step function, being 0 for $x < 1$ and 1 for $x > 1$. Thus the pair production rate does not depend on the target photon density, but only on the γ-ray production rate. In the case of large U_{ext}, when only the first order Compton scattering is important, analytical solutions are possible even taking into account thermal pair effects. These in fact influences the spectrum only at energies below threshold, because downscattering or diffusion are unimportant for hard photons, due to Klein Nishina decline of the scattering cross section. In this case the self consistent solution for the emergent spectrum can be understood in a very simple way.

Suppose to inject monoenergetic primary particles. Without pairs, $N(\gamma) \div \gamma^{-2}$, yielding a photon production rate $\dot{n}(x) \div x^{-3/2}$ (corresponding to $\ell(x) \div x^{-1/2}$). If all photons above threshold make pairs, $P(\gamma) \div \gamma^{-3/2}$. The steady energy density distribution will now be $N(\gamma) \div \gamma^{-3/2-1}$, in the range

of energies where pairs outnumber primary particles. Thus the new $\dot{n}(x) \div x^{-7/4}$, yielding $P(\gamma) \div \gamma^{-7/4}$, and so on. Continuing the argument, for the ith generation we have $P_i(\gamma) \div \gamma^{-\Gamma_i}$, $N_i(\gamma) \div \gamma^{-p}$, $\ell_i(x) \div x^{-\alpha_i}$, where $\Gamma_i = 2-1/2^i$, $p_i = 3-1/2^i$, and $\alpha_i = 1-1/2^{i+1}$ (Svensson 1985). Thus this simple argument explains why the final spectrum tends to approach the limiting value $\alpha=1$ for a large number of generations, and gives insights for other features:

i) For a given maximum energy of primary particles γ_{max} and soft photon x_o, only a finite number N of generations exist, and in general N will be small (Svensson 1986b)

$$N = \text{int}\left\{ \frac{\ell g\left(\frac{\ell g\, 2x_o/3}{\ell g(2x_o\gamma_{max}/3)} \right)}{\ell g\, 2} \right\} \qquad 3.11$$

ii) Different generations of pairs will dominate the emission at different energies, producing bends and kinks in the power law spectrum.

iii) The second reprocessing would further steepen the spectrum, producing breaks and tails.

Thus, even if the expected steepening by pairs effectively takes place, the final spectrum will not be a completely smooth power law and indistinguishable from i.e. that produced by a relatively steep injection distribution of primary particles.

It is important to note a general feature that pair dominated and non thermal sources should exhibit, resembling the case of steep injection in SSC models, due to the downscattering of hard photons. As shown by Sunyaev and Titarchuk (1980), this effect causes the spectrum to steepen between $x=1/\tau_T^2$ and $x=1$, by an amount that depends on the spatial distribution of the cool particles and photons. If both are uniform, the steepening is $\Delta\alpha=0.5$, and increases if photons are more concentrated in the center of the source. Thus the emergent spectrum, already steepened by the emission of the relativistic pairs, further steepens,

reaching a slope larger than unity for $x > 1/\tau_T^2$. As a consequence, $1/\tau_T^2$ is the energy where most of the luminosity comes out. It is easy to realize that τ_T increases with injected luminosity, so that non thermal plasma resemble thermal ones for what concerns the relation between the injected luminosity and the energy where most of it is emitted (which is of the order of kT/mc^2 for thermal radiation processes). In fact, for high ℓ, thermal plasmas in pair equilibrium have lower temperatures for higher luminosity (Svensson 1983), since the increased heating is shared by many more created pairs.

A different approach to the problem was chosen by Fabian (1984) and Fabian et al. (1986). They assume to inject monoenergetic electrons and soft photons and find the self consistent final spectrum numerically, including thermal pair effects. Their code is also used to follow the spectral changes of the source following istantaneous changes of the input parameters. While the results for steady state well agree with those of the previous authors, it is worth mentioning an interesting effect in the time dependent case.

Evaluating the annihilation timescale t_A from the annihilation rate gives $t_A = n_+/(\dot{n}_+)_A \sim R/(c\tau_T)$, which is, for $\tau_T > 1$, shorter than the light crossig time R/c or the escape time $R(1+\tau_T)/c$. Then a decrease in pair density, following a decrease in the primary particle injection (injected luminosity) can let the source become thin. Photons previously stored by diffusion can escape freely from the source producing an increasing flux, followed by the decrease corresponding to the lower injected luminosity. The reversed situation is similar: an increase in injected luminosity will correspond to an initial decrease in observed flux, as the photon trapping becomes more efficient. This situation can be the best opportunity to see the annihilation line, since hard photons are not trapped by diffusion, and can always escape.

4. Pair production in SSC models

When a magnetic field is present, relativistic electrons cool not only on a given, independent radiation energy density by the IC process, but also producing synchrotron photons. Thus, once pairs are created, their radiation contributes also to the soft radiation which in the models reviewed in the last chapter was fixed. We can estimate a minimum value of the magnetic field above which the energy density of synchrotron photons exceeds a given, external, radiation energy density

$$B^2/8\pi > U_{ext} \Longrightarrow B > 387(QL_{45}^{Ext})^{1/2}/R_{15}^2 \qquad 4.1$$

where Q is a dilution factor ($1>Q>0$), to take into account that L^{Ext} is generally produced in a different region of the source. For instance, we can think to the thermal radiation produced by an accretion disk, interacting with non-thermal electrons in a magnetized region at a distance d. In this case Q will approximately be $(R/d)^2$.

In the following, we restrict ourselves to cases in which QL^{Ext} can be neglected, and concentrate to the effects that pair production can have on the SSC model as I described in chapters 1 and 2.

A general consideration is in order. As pairs will contribute to the synchrotron emission and, in general, to the establishment of the steady energy distribution $N(\gamma)$, they will have important effects on the observed spectrum as a whole, not only in the X and γ-ray bands. Unfortunately, SSC models with pair production are more difficult to treat than the pure Compton models, because, in SSC, soft radiation is not fixed, and, moreover, cannot be approximated with a δ-function, as is the case for any peaked emission. We will show, however, that in some limited cases an analytical solution is possible.

4.1 The problem

Due to the high photon density in compact sources, the only important pair production process is photon photon interaction, with threshold and cross section given by eqs. 3.1 and 3.4. Photons above threshold are absorbed, and pairs created, at a rate

$$P(\gamma) = 4\dot{n}(2\gamma)\left[1 - \frac{1-e^{-\tau_{\gamma\gamma}(2\gamma)}}{\tau_{\gamma\gamma}(2\gamma)}\right] \qquad 4.2$$

where the factor 4 arises because two particles are produced in a pair production event and we assume $\gamma = x/2$ to be the energy of both particles. Here $\dot{n}(x)$ is the photon production rate at the energy x.

The inverse process, pair annihilation, occurs at a rate

$$(\dot{n}_+)_A = n_+ n_- (3/8)\sigma_T c f(\Theta) \qquad 4.3$$

where n_+ is the positron (electron) density and $f(\Theta)$ is a function of the dimensionless temperature $\Theta = kT/mc^2$

$$f(\Theta) \cong \left[1 + \frac{1}{2}\left(\frac{4\pi\alpha_f^2}{\Theta}\right)^{0.6} + \frac{4\pi\alpha_f^2}{\Theta}\right]^{\frac{1}{2}}\left[1 + \frac{2\Theta^2}{\ln(1.12\Theta + 1.3)}\right]^{-1} \qquad 4.4$$

(Svensson 1986b), which has the asymptotic behaviours

$$f(\Theta) \longrightarrow \frac{\ln 2\Theta}{2\Theta^2} \quad ; \quad \Theta \gg 1 \qquad 4.5a$$

$$f(\Theta) \longrightarrow 2\alpha_f(\pi/\Theta)^{1/2} \quad ; \quad \Theta \ll 1 \qquad 4.5b$$

For temperatures of interest here, $f(\Theta)$ is of order unity. A thermal distribution is assumed, since the slowing down timescale for an energetic particle to reach the temperature Θ and thermalize is shorter than the annihilation time t_A (Svensson 1986b)

$$t_A = n_+/(\dot{n}_+)_A = \frac{16}{3f(\theta)} \frac{R}{c} \frac{1}{\tau_T} \qquad 4.6$$

where $\tau_T = 2n_+ \sigma_T R$ is the pair Thomson optical depth, computed balancing pair production and annihilation rates (Zdziarski 1986)

$$\tau_T = \left[\frac{16 \sigma_T R^2}{3c f(\theta)} \int_1^{\gamma_{max}} P(\gamma) d\gamma \right]^{1/2} \qquad 4.7$$

The fate of a typical positron created with an energy γmc^2 is to radiatively cool down to subrelativistic energies, where it thermalizes through Coulomb collisions before annihilating.

The pair production rate acts as a continuous injection of secondary particles, and the continuity equation takes the form

$$N(\gamma) = \frac{3mc \gamma^{-2} \int_\gamma^{\gamma_{max}} [Q_0(\gamma') + P(\gamma')] d\gamma'}{4 \sigma_T \left[U_B H(\gamma - \gamma_t) + \int_{x_t}^{3/4\gamma} U_r(x) dx \right]} \qquad 4.8$$

Note that, for $\tau_T > 1$, photon diffusion takes place, enhancing the radiation energy density up to x=1 by the factor $\sim 1+\tau_T$.

4.2 The case of one generation of pairs

4.2a The model

General solutions of eq. 4.8 must be worked out numerically, but a number of approximations are possible in limited cases, which allows for an analytical solution. Here I will follow the procedure of Ghisellini (1986).

i) we will take into account only the first order Compton scattering, requiring $U_B > U_r^s$, and flat injections.

ii) We will consider sources compact enough to absorb all photons of energy x>2 through collisions with photons of energy x'=2/x. We assume that the electrons and positrons thus created both have $\gamma = x/2$. This requires $\tau_{\gamma\gamma}(1) > 1$, and

makes the pair production rate independent on the target photon density:

$$P(\gamma) \cong 4\dot{n}(2\gamma) \qquad 4.9$$

iii) We will consider cases in which only one generation of pairs is produced, requiring that pairs cannot scatter synchrotron photons above threshold. This condition reads

$$\gamma_{max} < 1.27\times10^{4}B^{-3/10} \qquad 4.10$$

Even if this condition is violated, the emission by the pairs above x=2 is not important as long as it is smaller than the emission by the primary particles, and this occurs for a much larger value of γ_{max}. On the other hand, primary particles produce photons above threshold by the first order IC process if

$$\gamma_{max} > 2.65\times10^{3}B^{-1/4} \qquad 4.11$$

iv) We assume complete Thomson cooling, which requires

$$\gamma_{max} < 2.91\times10^{4}B^{-1/3} \qquad 4.12$$

but since we already assumed $U_B > U_r$, the effect of neglecting the Klein Nishina cooling is not important, and larger value of γ_{max} can be considered.

v) For simplicity, we assume a monoenergetic injection of primary particles at γ_{max}

$$Q_0(\gamma) = A\,\delta(\gamma-\gamma_{max}) \qquad 4.13$$

Similar results should be obtained for flat (s<1) power law injections.

Since we consider cases in which the synchrotron process dominates the cooling, the power absorbed at x>2 (which

derives from IC) is small compared to the synchrotron one. The absorbed power will be redistributed at all energies, but will not largely affect the total synchrotron energy density. In other words, pairs will not contribute to the emission close to the maximum energy of the primary synchrotron spectrum, x_{smax}. Taking into account only synchrotron and first order IC cooling we have

$$N(\gamma) = \frac{3mc}{4\sigma_T U_B} \frac{\gamma^{-2}}{H(\gamma-\gamma_t) + U_r^s/U_B} \left\{ A + \int_{\gamma}^{\gamma_{max}} P(\gamma')d\gamma' \right\} \quad 4.14$$

$$U_r^s = \frac{1}{2} U_B \left[\sqrt{\varphi+1} - 1 \right] \quad 4.15$$

$$\varphi = 4 \frac{U_i}{U_B} (1+\tau_T) \quad 4.16$$

$$U_i = \frac{3}{4} \frac{3 L_i}{4\pi R^2 c} \quad 4.17$$

where L_i is the injected luminosity in relativistic electrons. Above threshold, emission by pairs does not contribute. Thus, in calculating the Compton photon production rate for x>2, we can neglect the term involving pairs in eq. 4.14 and then find $P(\gamma)$ analytically. The solution is

$$P(\gamma) = \frac{\sqrt{2}c}{3 a_o \sigma_T} \frac{x_B^{3/2}(1+\tau_T)}{R \gamma_{max}^2} \left(\frac{U_i}{U_B}\right)^2 f^2(\varphi) \gamma^{-3/2} \ln\left(\frac{\gamma_p}{\gamma}\right) \quad 4.18$$

$$f(\varphi) = \frac{\sqrt{\varphi+1} - 1}{\varphi} \quad 4.19$$

where a_o is the Bohr radius, $a_o = 5.29 \times 10^{-9}$ cm. Note that $P(\gamma)$ is approximately a power law. The logarythmic term enters here because pairs are created in the tail of the IC spectrum, where we do not have a pure power law. The steady state energy distribution for the secondary pairs only is

$$N^p(\gamma) \div \gamma^{-2} \int_{\gamma}^{\gamma_p} (\gamma')^{-3/2} \ln(\gamma_p/\gamma') d\gamma' \quad 4.20$$

where γ_p is the maximum Lorentz factor of the pairs. Since our conditions prevent γ_p to be very large, the upper limit cannot be neglected, introducing another correction to a pure power law for $N^p(\gamma)$, making it steeper than $\gamma^{-5/2}$ for γ approaching γ_p.

4.2b Effects of thermal pairs

High optical depth for γ-γ interactions necessary imply high scattering optical depths τ_T of the cool pairs. To derive in a simple way the equilibrium Compton temperature at which they thermalize, we balance energy losses and gain. As discussed in chapter 2, downscattering will heat the pairs, while they cool upscattering synchrotron photons producing a tail above x_{smax}, with a spectral index α_{th} defined by eq. 2.38. Taking into account that downscattering steepen $\ell(x)$ by a factor $\Delta\alpha=0.5$ and $U_r(x)$ by a factor $\Delta\alpha\cong 1$ between $1/\tau_T^2$ and 1, we have

$$(e^y-1)\int_{x_t}^{x_{smax}} \ell(x)dx \cong \int_{1/\tau_T^2}^{1} \ell(x)(1-x^{-1})dx \qquad 4.21$$

where the Comptonization parameter $y=4\theta\tau_T^2$. In the case in which the IC radiation by primary particles dominates the emission above $1/\tau_T^2$ we have

$$\theta \cong \frac{1}{4\tau_T^2}\ln\left[1+\frac{\sqrt{\gamma_p+1}-1}{4\sqrt{2\gamma_p}}\ln\left(\frac{x_{smax}}{x_t}\right)\left(1-\frac{1}{\tau_T}\right)^2\right] \qquad 4.22$$

Another interesting parameter is the pair yield ξ, which is defined as the ratio of the energy in rest mass of pairs to the injected energy. Measuring the efficiency of converting into pairs the injected luminosity, ξ is directly related to the annihilation line luminosity. For monoenergetic injections

$$\xi = \frac{\int_1^{\gamma_p} P(\gamma)\,d\gamma}{A\,\gamma_{max}} = \frac{\pi}{4}\frac{\tau_T^2}{\ell_i} \qquad 4.23$$

where ℓ_i is the dimensionless injected luminosity. It is interesting to note that, for a given ℓ_i, τ_T and ξ have a maximum when

$$B = 1.2\times10^{15}\,\gamma_{max}^{-4} \qquad 4.24$$

Using this relation, we find that the maximum ξ ranges from 8.2% to 1.5% as U_r/U_B decreases from 1 to 0.1.

4.2c An example

Our model is completely specified by four parameters: the radius of the source R, the magnetic field strength B, the energy of the injected primary electrons γ_{max} and the injected luminosity L_i, or equivalently, ℓ_i.

In fig. 8, $\ell(x)$ is plotted separately for each contribution to the final spectrum for the following choise of parameters: $L_i=10^{47}$erg/s, B=4000 G, $\gamma_{max}=1000$, and $R=3\times10^{15}$cm, corresponding to $\ell_i=900$.

From the figure is apparent that pair production effects strongly influence the shape of the spectrum, even if most of the luminosity comes from emission produced by the primary electrons. Pairs are marginally important in the lower energy part of the synchrotron spectrum, due to the fact that radiation is heavily self-absorbed in the energy range where synchrotron emission by the pairs could dominate. For the IC spectrum we have four contributions, corresponding to the scattering between primary electrons or pairs with their synchrotron photons. For the chosen values of fig. 8, the scattering of pairs off primary electron synchrotron photons is dominant up to $x=10^{-2}$. In fig. 8 we plot also the comptonized spectrum calculated using eqs. 2.38 and 4.22. The optical depth for scattering is $\tau_T\cong7.8$, while the equilibrium Compton temperature is $\Theta\cong9.8\times10^{-4}$, giving $\alpha_{th}\sim5$. At $x=1/\tau_T^2\cong1.6\times10^{-2}$, the spectrum steepens due

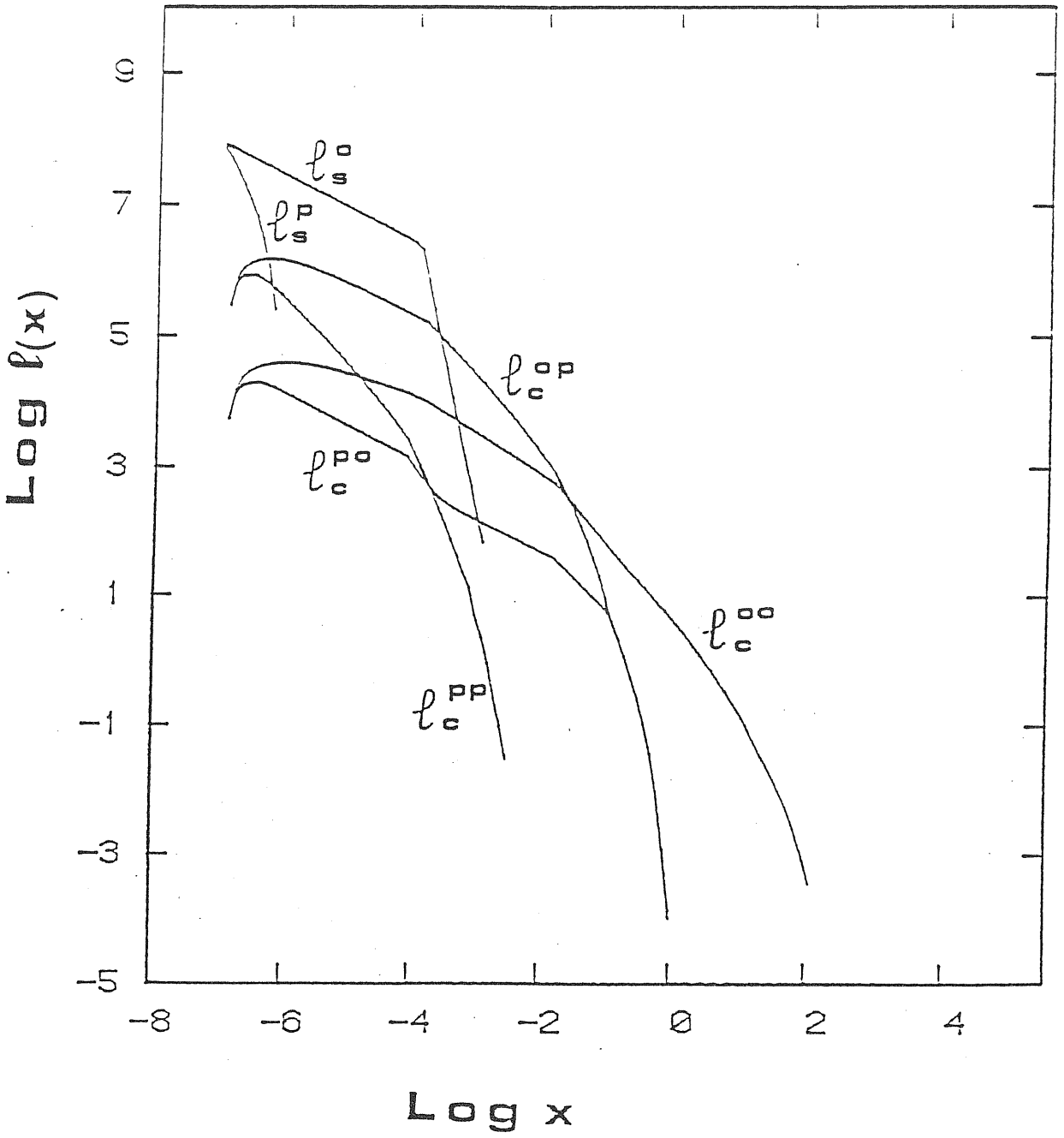

Fig. 8 SSC spectrum corresponding to monoenergetic injection of electron with γ=1000. R=3x10^{15}cm., L=10^{47}erg/s, B=4000 G. x is the dimensionless photon energy measured in units of mc^2. The labels correspond to:

ℓ_s^0=primary synchrotron and Comptonized spectrum made by the thermal pairs.

ℓ_s^p=synchrotron made by pairs

ℓ_c^{00}=IC from primary electrons scattering primary synchrotron

ℓ_c^{0p}=IC from pairs scattering primary synchrotron

ℓ_c^{p0}=IC from primary electrons scattering pair synchrotron

ℓ_c^{pp}=IC from pairs scattering pair synchrotron

to downscattering. Even if we assumed that each photon above x=2 makes pairs, a high energy tail is present, due to the emission from the surface layers of the source. For energies x greater than 2, the emerging radiation has a slope $\alpha(x)=2\,\alpha(2/x)$ (Svensson 1984). Further absorption is expected for this high energy radiation passing the X-ray photosphere, but it is not shown.

In fig. 9 the sum of all the contributions to $\ell(x)$ of the previous case is compared with the SSC spectrum deriving from a source with the same size and magnetic field, but with $\gamma_{max}=333$ and $L=3.3\times10^{46}$ erg/s (i.e. same number of primary electrons are injected as in the previous example). In the latter case, no photons can be emitted in the first order IC above x=2, and no pair can be produced. Note that the IC spectrum has <u>not</u> the same shape as the synchrotron one, due to the discontinuity of $N(\gamma)$ caused by selfabsorption.

Supposing that in the source γ_{max} istantaneously increases from 333 to 1000, all other quantities remaining the same, the observed spectrum changes as in fig. 9. At 1 keV, an increase of a factor of $\sim$4 in the monochromatic flux density will be observed, in a time that is the escape time from the source: $\Delta t\cong(1+\tau_T)R/c\cong10$ days. At the same energy, the spectral index steepens from $\alpha_x=0.85$ to $\alpha_x=1.1$. A larger increase both in intensity and spectral index is expected in the comptonized region of the spectrum, that in fig. 9 dominates the emission between $x_{smax}=1.2\times10^{-4}$ and $x=3\times10^{-4}$.

It is important to note that further effects can occur on timescales shorter than the escape time. In fact the enhanced photon trapping can initially decrease the observed luminosity in the example made, as shown by Fabian et al. (1986). On the other hand, since pairs annihilate in the timescale shorter than the crossing time R/c for $\tau_T>1$, more rapid variability is expected when the source switches from a pair dominated to a pairfree state. The minimum observable

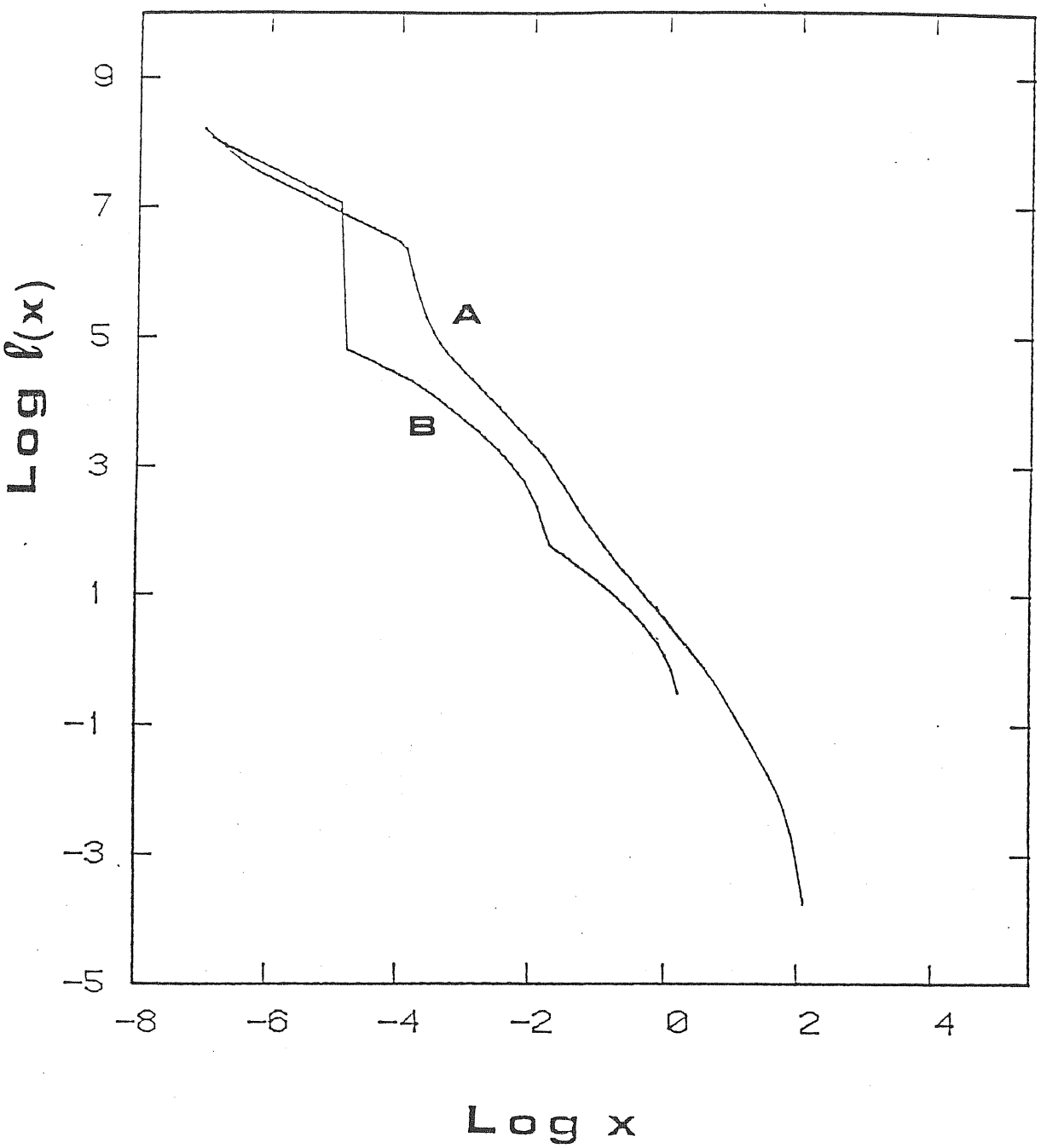

Fig. 9 Curve A is the sum of all contributions shown in fig.1.
Curve B is the SSC spectrum corresponding to monoenergetic injection of electrons with γ=333. L=3.3x10^{46}erg/s, and B and R as in fig. 1.

variability timescale is however R/c.

4.2d Discussion

In fig. 10 the region of the parameter space allowed for our model is shown for $R=3\times10^{15}$cm and $L_i=10^{47}$erg/s ($\ell_i\cong900$), and for monoenergetic injections at γ_{max}. It is constrained by the requirements: i) $U_r^s/U_B<1$ (thick line), ii) the maximum energy of the first order IC spectrum is greater than 2 (dotted line), and iii) the optical depth for γ-γ interactions, $\tau_{\gamma\gamma}(x)$, is greater than unity at the threshold $x=2$ (dashed line). Also shown is the function corresponding to the maximum pair yield ξ_{max} (dash-dotted line) and the line corresponding to $\gamma_{max}x_{smax}=3/4$, that is the limit for complete Thomson cooling (thin line). Note that U_r^s is increased by the trapping pairs, so that the limit $U_r^s/U_B = 1$ does not correspond to a straight line in fig. 10.

In general, for any given γ_{max}, the importance of pairs increases lowering the value of magnetic field, as a larger fraction of the injected luminosity comes out at high energies. In particular, for $U_r^s/U_B<1$ and low γ_{max}, very few pairs should be present in the source, produced by the second and higher orders IC scatterings, that becomes important only for $U_r^s/U_B>1$.

On the other hand, for high γ_{max}, and $U_r^s/U_B<1$, $\tau_{\gamma\gamma}(x)$ becomes greater than unity only at $x>>2$. Furthermore, Klein Nishina effects start depressing the radiation emitted at high energies, even for the first order IC process. Both these effects decrease the number and the importance of the produced pairs compared to the injected particles.

The region of parameter space in which pairs are more important is the one between the 'threshold line' and the line beyond which Klein Nishina effects becomes to affect the emission of the first order IC. Part of this region fulfills the requirements to derive the final self consistent spectrum analytically, and we have seen in the

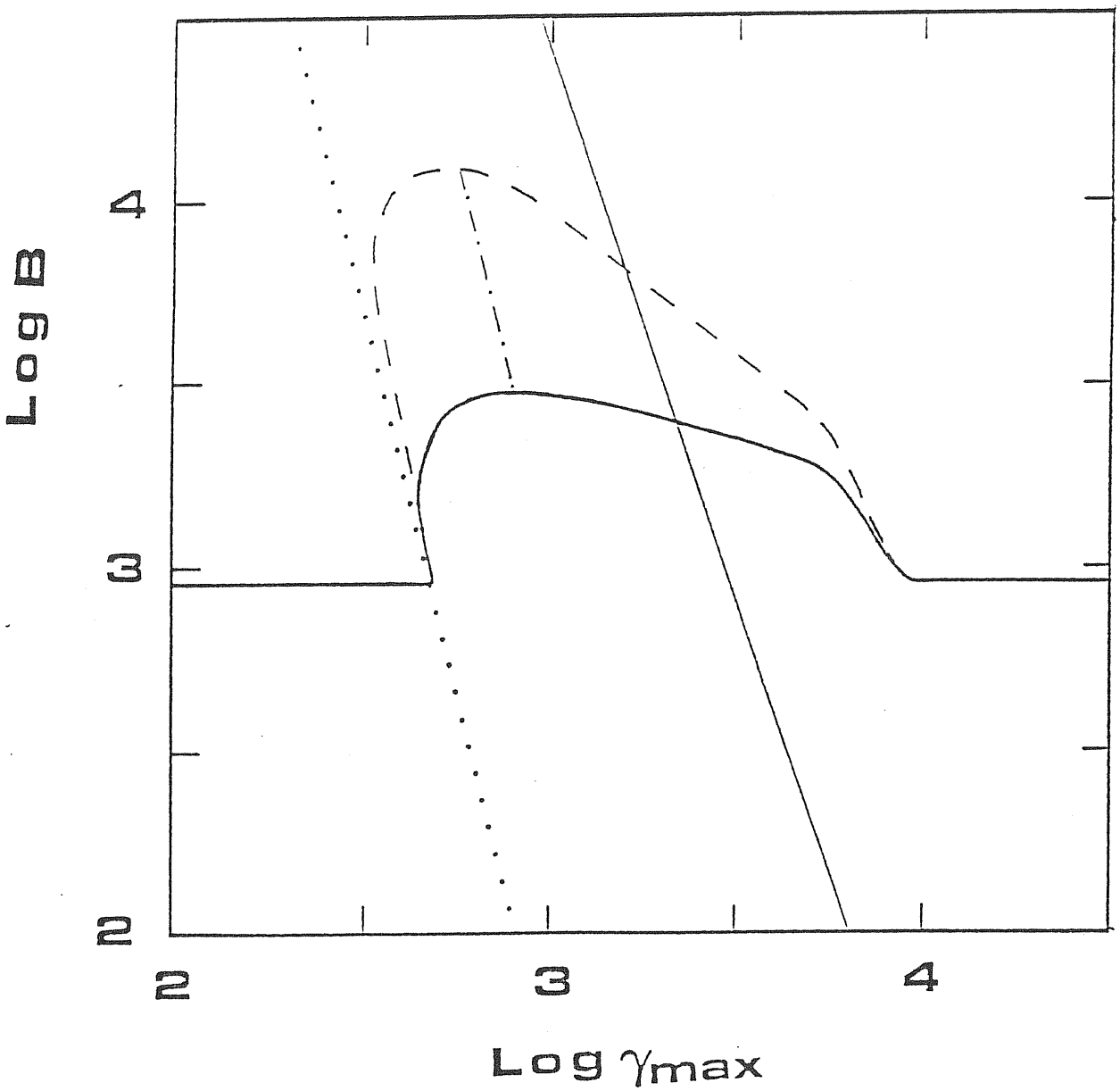

Fig. 10 The parameter space for $L_i=10^{47}$ erg/s and $R=10^{15}$ cm, corresponding to $\ell_i=900$. Monoenergetic injection at ℓ_{max} is assumed
thick line: $U_r^s/U_B = 1$;
dotted line: $\gamma_p = 1$
dashed line: $\tau_{\gamma\gamma}(2) = 1$;
dash dotted line: $\ell = \ell_{max}$;
thin line: $\gamma_{max} x_{smax} = 3/4$.

example of fig. 8 how pairs modify the emergent radiation from the source.

For $U_r^s/U_B<1$, pairs do not affect the region of the spectrum where most of the luminosity comes from, but have a great influence on the whole X-ray band. For $U_r^s/U_B>1$, we expect pairs to play an even greater role in reprocessing radiation from higher to lower energies, eventually leading to a spectrum characterized by the spectral index $\alpha \cong 1$ in all bands, as suggested first by Bonometto and Rees (1971). Here, with only one generation of pairs, the spectral index in particular bands (i.e. X-rays) can be steeper than 1, either because of logarithmic dependences of $P(\gamma)$, or because of up- and down-scattering.

In fig. 10, the 'threshold line' marks the boundary between a region in which the source is almost pair free, and a region in which high densities of pairs can be reached, with all the effects described above. Starting from this pairfree region, a small change in γ_{max} can produce dramatic effects in the X-ray band. We would like to stress the possible relevance of this threshold crossing effect as a cause of large observed variability in AGNs, present in both soft and hard X-ray bands. As can be seen in fig. 10, for particular values of the magnetic field a change in γ_{max} can even change the dominant cooling mechanism, producing large variability also in the synchrotron spectrum, besides the changes induced by the synchrotron radiation emitted by the pairs.

The derived analytic solution is valid for a small region of the parameter space, due to the requirement of having U_r^s/U_B less than, but close to, unity, in order to have high enough X-ray compactness to absorb all photons above threshold, still neglecting higher order Compton scatterings. However this solution can be useful in understanding numerical results in the other regions of the parameter space, and particularly those correspondent to $U_r^s/U_B>1$, where pairs are expected to play an even greater role.

Conclusions

In this study, it is found:

i) Assuming no reacceleration, and considering only synchrotron and Compton cooling, an injected distribution of relativistic particles reaches steady state in a time t_{cool} that in compact sources is shorter than the escape or the annihilation time. The optical depth τ_c of the relativistic particles cannot be larger than unity, independent of the number of injected particles, and approaches unity in the case of steep injections (s>2).

ii) In the case of flat injections and dominant magnetic field, ($U_B/U_r>1$), the IC spectrum is steeper than the synchrotron one in a large range of energies.

iii) The spectral index of a steady, uniform, compact source without reacceleration can be flatter than 0.5 only if the Klein Nishina dimming is important, requiring $U_r/U_B>1$ and large γ_{max}.

iv) In the case of steep injections (s>2), Compton losses always dominate the cooling, independently on the ratio U_B/U_r, provided that the cooling time is shorter than the escape or the annihilation time, and that no reacceleration is present. In this case the spectral index of the emitted spectrum is always flatter than unity below $x=1/\tau_T^2$, and steeper injections correspond to flatter spectra. In these conditions cool particles are always important as their Thomson optical depth $\tau_T \gtrsim 0.3$. Even for large dimensionless compactnesses ℓ, pair photoproduction is not important in this case, as the γ-ray spectrum is steep

v) Including pair production in SSC models requires, in general, a numerical approach, but in a restricted range of

parameters analytical solutions are possible. In this range, the effects of both relativistic and thermal pairs have been shown. It is found than in particular cases the source can switch from a pairfree state to another state in which copious pair production takes place, with important consequences on the intensity and spectral shape variability.

Acknowledgments

It is a pleasure to thank my supervisors Roland Svensson and Marek Abramowicz for their continuous encouragement and scientific guidance, and Laura Maraschi, Aldo Treves, and Piero Madau for very helpful discussions.

References

Blumenthal, G.R., and Gould, R.J., 1970. Rev. of Mod. Physics, **42**, 237

Bonometto,S., and Rees, M.J., 1971. Mon.Not.R.astr.Soc., **152**, 21

Fabian, A.C.: in X-ray and UV emission from Active Galactic Nuclei edited by J. Trumper and W. Brinkmann (Max Plank, Garching, 1984) p. 232

Fabian, A.C., Blandford, R.D., Guilbert, P.W., Phynney, E.S., and Cuellar, L., 1986. Mon. Not. R. astr. Soc., **221**, 931

Ghisellini, G., Maraschi, L., and Treves, A., 1985. Astr. Astroph., **146**, 204

Ghisellini, G., Maraschi, L., Tanzi, E.G., and Treves, A., 1986, to appear in Astroph. J., Nov. 1

Ghisellini, G., 1986, to appear in Mon. Not. R. astr. Soc.

Hoyle, F.R.S., Burbidge, G.R., and Sargent, W.L.W., 1966. Nature, **209**, 751

Jones, T.W., O'Dell, S.L., and Stein, W.A., 1974. Astrophys. J. **188**, 353

Kazanas, D., 1984. Astroph. J., **287**, 112

Kellerman, K.I., and Pauliny Toth, I.I.K., 1969. Astroph. J. (Lett.), **155**, L71

Madau, P., Ghisellini, G., and Persic, M., 1986. to appear in Mon. Not. astr. Soc.

Madejski, G.M., and Shwartz, D.A., 1983. Astroph. J., **275**, 467

Maraschi, L., Tanzi, E.G., and Treves, A., 1983. 24th Liege Coll., p. 437

Rees, M.J., 1967. Mon. Not. R. astr. Soc., **137**, 429

Stepney, S., 1983. Mon. Not. astr. R. Soc., 1983, **202**, 467

Sunyaev, R.A., and Titarchuk, L.G., 1980. Astr. Astrophys., **86**, 121

Svensson, R., 1984. Mon. Not. R. astr. Soc., **209**, 175

Svensson, R.: in X-ray and UV emission from Active Galactic Nuclei edited by J. Trumper and W. Brinkmann (Max Planck, Garching, 1984) p. 152

Svensson, R.: in Radiation hydrodynamics in Stars and Compact Object, IAU Coll. 89, 1986a. in the press.

Svensson, R., 1986b. preprint

Tucker, W.H., 1983. Astroph. J., **271**, 531

Wandel, A., and Mushotzky, R.F., 1986. Astroph. J. (Lett.), **306**, L61

Zdziarski, A.A., and Lightman, A.P., 1985. Astrophys. J. (Lett.), **294**, L79

Zdziarski, A.A., 1986. Astrophys. J., **305**, 45

Zdziarski, A.A., and Lamb, D.Q., 1986. preprint